May 2024

Corrections to Kerr Black Holes in Modified Gravity

Carmen López Jurado

Division of Particle and Nuclear Physics, Department of Physics, Lund University

Master thesis supervised by Johan Bijnens

LUND
UNIVERSITY

Abstract

This thesis studies the effects of Higher-Derivative Gravity, in an Effective Field Theory format, on the properties of a rotating black hole. In particular, it corrects the Hilbert-Einstein action with curvature invariants that contain six and eight derivatives. The resulting Equations Of Motion are first derived, and then solved with an ansatz that permits the study of black holes with an arbitrarily high spin χ. The last section of this work is divided into two parts. The first one focuses on the effects of the action corrections on the outer horizon. Here, the Rigidity Theorem is checked, and the angular velocity, surface gravity, area, and deformation are examined. The second part focuses on the effects of the corrections on the ergosphere, where it is checked that the poles touch the horizon, and the deformation is examined. The main conclusion is that the eight-derivative results behave quite differently from their six-derivative counterparts, especially concerning the horizon and ergosphere deformations.

Populärvetenskaplig beskrivning

General Relativity is Albert Einstein's theory of gravity, which he proposed in 1915. It improves upon Newton's theory of gravity and has been successfully tested over the years. Even though it is a very successful theory, it is incomplete because it has a few flaws. For example, it predicts that the center of a black hole is infinitely dense, which is not possible! Because of this, "relativists" have been working on improving General Relativity for many years.

All results in modern physics theories come from a formula called the action. By modifying this formula, the theory and its predictions are also modified. Based on intricate mathematical and physical arguments, relativists have been modifying the action of General Relativity in many different ways.

This thesis focuses on improving the theory of gravity by modifying the action in one of those ways. The resulting modified gravity is then applied to the case of a rotating black hole. The final results of this thesis mainly focus on some properties of the event horizon, that is, the boundary beyond which everything is drawn into the center of the black hole. We can use the theory presented in this thesis to illustrate the shape of the event horizon of the black hole, see the figure below, where x and z make up the right side of the horizon in question, and the different coloured shapes correspond to slightly different modifications of the theory, leading to different horizon sizes.

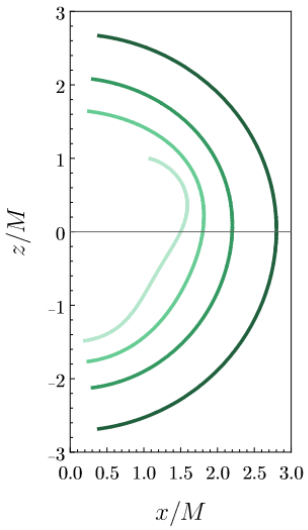

Studies like this are more useful than one might think. These results can be compared with the data coming from gravitational wave observatories. Once the comparison is made, the General Relativity modifications can be discarded or accepted until a definite Theory of Gravity is found. These theories not only give us a better understanding of the Universe, but might also lead to exciting technological advances, such as interstellar travel close to the speed of light, or even travels to the future.

Contents

1 Introduction **6**

2 Modifying the Hilbert-Einstein Action **8**

2.1 Overview of Effective Field Theory 9

2.2 Higher-Derivative Gravity as an Effective Field Theory 9

3 Reproducing the equations of motion **11**

3.1 Deriving the Euler-Lagrange Equations 11

3.2 Applying the Euler-Lagrange Equations 13

4 Solving the equations of motion **15**

4.1 Perturbing the equations of motion 15

4.2 Correcting the Kerr metric 17

5 Properties of the corrected Kerr Black Hole **20**

5.1 Horizon 20

5.1.1 Killing horizon 21

5.1.2 Angular velocity 22

5.1.3 Surface gravity 24

5.1.4 Geometry 25

5.1.4.1 Area 25

5.1.4.2 Shape 26

5.2 Ergosphere 29

6 Conclusions **35**

A Reproduction of the EOM associated to the eight-derivative correction $\mathcal{C}\tilde{\mathcal{C}}$ **37**

B First-order perturbation of the Einstein tensor **39**

C H_i functions in the metric corrections **40**

D Coefficients of the corrected Kerr Black Hole's properties **42**

List of acronyms

GR General Relativity
EH Hilbert-Einstein
MG Modified Gravity
EFT Effective Field Theory
EL Euler Lagrange
EOM Equations Of Motion
EFE Einstein Field Equations

List of Figures

1 Corrections to the angular velocity associated with the six and eight-derivative corrections to the action. 23

2 Corrections to the surface gravity associated with the six and eight-derivative corrections to the action. 25

3 Corrections to the area of the horizon associated with the six and eight-derivative corrections to the action. 26

4 Isometric embedding of the Kerr horizon and its deformations due to the even part of the six-derivative corrections. The mass was set to one, the black dashed curve is the Kerr horizon, and from light to darker purple, the value of the couplings is $\frac{\ell^4}{M^4}\lambda_{\rm ev} = -0.4, -0.2, 0.2, 0.4$. The left subfigure was generated with $\chi = 0.65$ and an H_i order of fifteen, and the right subfigure was generated with $\chi = 0.18$ and an H_i order of twenty-five. 28

5 Isometric embedding of Kerr horizon's deformations due to the odd part of the six-derivative corrections. The coupling $\frac{\ell^4}{M^4}\lambda_{\rm odd}$ was set to 0.6, and from light to darker green, the value of the mass is $M = 0.75, 0.9, 1.1, 1.4$. The left subfigure was generated with $\chi = 0.65$ and an H_i order of fifteen, and the right subfigure was generated with $\chi = 0.18$ and an H_i order of twenty-five. 29

6 Isometric embedding of the Kerr horizon and its deformations due to the eight-derivative corrections up to order twenty-five. The left and middle subfigures show the deformations related to ϵ_1 and ϵ_2, respectively. For both of them, the mass was set to one, $\chi = 0.18$, and the black dashed curve is the Kerr horizon. From light to darker purple, the value of the couplings is $\frac{\ell^6}{M^6}\lambda_{\rm ev} = -0.4, -0.2, 0.2, 0.4$ and $\frac{\ell^6}{M^6}\lambda_{\rm ev} = -4, -2, 2, 4$, respectively. The right subfigure shows the deformations related to ϵ_3. It was generated with $\chi = 30$, an H_i order of twenty-five, $\frac{\ell^6}{M^6}\epsilon_3 = 0.6$, and masses $M = 0.75, 0.9, 1.1, 1.4$. 30

7 Isometric embedding of the Kerr ergosphere and its deformations due to the even part of the six-derivative corrections. The mass was set to one, the black dashed curve is the Kerr horizon, and from light to darker purple, the value of the couplings is $\frac{\ell^4}{M^4}\lambda_{\rm ev} = -0.6, -0.3, 0.3, 0.6$. The left subfigure was generated with $\chi = 0.65$ and an H_i order of fifteen, and the right subfigure was generated with $\chi = 0.18$ and an H_i order of twenty-five. 32

8 Isometric embedding of Kerr ergosphere's deformations due to the odd part of the six-derivative corrections. The coupling $\frac{\ell^4}{M^4}\lambda_{\rm odd}$ was set to 0.6, and from light to darker green, the value of the mass is $M = 0.75, 0.9, 1.1, 1.4$. The left subfigure was generated with $\chi = 0.65$ and an H_i order of fifteen, and the right subfigure was generated with $\chi = 0.25$ and an H_i order of twenty-five. 33

9 Isometric embedding of the Kerr ergosphere and its deformations due to the eight-derivative corrections up to order twenty-five. The left and middle subfigures show the deformations related to ϵ_1 and ϵ_2, respectively. For both of them, the mass was set to one, $\chi = 0.18$, and the black dashed curve is the Kerr horizon. From light to darker purple, the value of the couplings is $\frac{\ell^6}{M^6}\epsilon_1 = -0.6, -0.3, 0.3, 0.6$ and $\frac{\ell^6}{M^6}\epsilon_2 = -2, -1, 1, 2$. The right subfigure shows the deformations related to ϵ_3. It was generated with $\chi = 0.25$, an H_i order of twenty-five, $\frac{\ell^6}{M^6}\epsilon_3 = 0.6$, and masses $M = 0.75, 0.9, 1.1, 1.4$. . . . 34

1 Introduction

General Relativity (GR) is a successful theory, not only because it improves Newton's Law of gravitation and generalizes special relativity, but also because it agrees with numerous precision tests [1]. Two recent achievements include the detection of gravitational waves [2], and the generation of an image of a black hole [3].

GR is a complete theory at a classical level. However, it needs to be improved for spacetimes of large curvature [4]. One problem in this regime is the black hole singularities [4], of which Albert Einstein was aware [5]. It has been one of the motivations for relativists to work on a high-curvature successor to GR [4], opening up the Modified Gravity (MG) field.

Probably the most popular MG modality is the quantization of gravity, which is one of the hardest physics problems ever due to its theoretical complexity and apparent experimental impossibility. An alternative way to modify GR consists of adding Higher-Derivative corrections to the GR action (see section 2). Numerous works listed in [6] suggest that the effects of these additional terms are significant at high energies, eliminating the GR singularities more effectively than other approaches.

A side effect of these Higher Derivative theories is that the properties of black holes at the horizon and ergosphere deviate from GR results. Studying these deviations is useful, as they can be compared with data from LIGO, VIRGO, Event Horizon Telescope[1], or other present and future initiatives, allowing for setting bounds to these gravity theories [6]. This is indeed the ultimate objective of Ref. [6], which derives properties of the horizon and ergosphere, as well as the photon rings,[2] of a rotating black hole. Although not of interest to this thesis, this reference also studies a quantum property of black holes called scalar hair.

Ref. [6] is novel in Modified Gravity for two reasons. i) It considers String Theory corrections, a Quantum Gravity candidate, along with a generalization of Higher-Derivative theories. The latter was accomplished by adding up curvature invariants containing six partial derivatives following the Particle Physics method Effective Field Theory (EFT) (see Section 2 below). ii) Earlier analytical applications of MG theories to rotating black holes expand their corresponding metric in a power series of the rotational spin. Previously, it was difficult to solve for the metric of these theories. Therefore, these works only include a few terms in the expansion, reducing their validity to small values of spin or slowly rotating black holes; see references in [6]. However, astrophysical black holes usually have a relatively high spin. Reference [6] is the first analytical work that provides a methodology for solving the metrics in Higher-Derivative theories for an arbitrarily high spin. In addition, the solution is used to study the properties that become significant at high spins and have been disregarded previously, like the shapes of the horizon and ergosphere.

[1] LIGO [7] and VIRGO [8] are gravitational wave detectors settled in USA and Italy, respectively. The Event Horizon Telescope [9] is a global network of radio telescopes that aim to observe black hole event horizons.

[2] Photon rings are light rays at the equatorial plane

This thesis intends to extend Ref. [6] by adding the eight-derivative invariants, described in [10], to the Higher-Derivative generalization of the former. It does not consider String Theory nor studies scalar hair, but except for that, it follows the steps of this former work from the construction of the action to the study of the ergosphere. Chapter 2 gives a brief overview of EFT, explains how Ref. [6] uses this method to generalize Higher-Derivative Gravity, and presents the action used in this thesis. Chapter 3 explains how the suitable Euler Lagrange (EL) equations were derived and how the Equations Of Motion (EOM) in Refs. [6, 10] were reproduced. Chapter 4 explains how the metric of this thesis was found. First, it focuses on how the EOM were perturbed, and then, how the ansatz for the case of a rotating black hole, based on [6], was derived and solved. Chapter 5 uses this corrected metric to derive and discuss the following properties of the rotating black hole at a classical level: nature of the horizon, horizon angular velocity, horizon surface gravity, horizon area, horizon shape, and the ergosphere shape. The last chapter is the conclusion of this thesis. It summarises chapters 2 to 4, highlights the most important details about the properties of the black hole, and offers an outlook. This thesis also contains an appendix. Part A shows the reproduction of one of the terms in the EOM, part B sketches the first-order perturbation of the Einstein tensor for a general curved vacuum spacetime according to [11], part C shows the H_i expansions that belong to the metric corrections up to second order in spin, and part D shows the expansions that belong to the properties of the rotating black hole.

Regarding references that work with the eight-derivative invariants, Ref. [10] studies their effect on non-rotating, spherically symmetric vacuum solutions, as well as slowly rotating black holes. Thus, it uses a metric ansatz different from this thesis. A reference that uses the same ansatz is [12], which is indeed a continuation work of Ref. [6]. However, the former reference focuses on a well-known characterization of gravitational waves emitted by a remnant black hole after a binary merge. Nevertheless, the metric correction associated with the eight-derivative invariants, which was derived and solved independently using the methods in [6], agrees with the continuation work. With this in hand, the following lists specify this thesis reproduced and original results. Any other result was taken from a source, which is cited where applicable.

- Reproduced results: EOM Eqs. (3.22) and (3.23), perturbed EOM Eqs. (4.42) and (4.43), functions $H_i^{(6)}$ and $H_i^{(8)}$ in the corrected metric (appendix C), Rigidity Theorem verification, Kerr horizon angular velocity and its six-derivative correction Eqs. (5.63) and (D.1), Kerr horizon surface gravity and its six-derivative correction Eqs. (5.67) and (D.4), Kerr horizon area and its six-derivative correction Eqs. (5.71) and (D.7).

- Original results: EL equations Eq. (3.20), eight-derivative correction to the horizon angular velocity Eqs. (5.63), (D.2) and (D.3), eight-derivative correction to the horizon surface gravity Eqs. (5.67), (D.5) and (D.6), eight-derivative correction to the horizon area Eqs. (5.71), (D.8) and (D.9), horizon shapes Figs. 4 to 6, ergosphere shapes Figs. 7 to 9.

Finally, note that latin indices of tensors run from 0 to 3 in this thesis.

2 Modifying the Hilbert-Einstein Action

In theoretical physics, the choice of action is crucial, as any other result or observable is derived from it. The action of GR reads

$$S = \frac{1}{16\pi G} \int d^4x \sqrt{-g} R \,, \tag{2.1}$$

which yields the Einstein Field Equations (EFE) via the EL equations. Moreover, it takes the name of Einstein-Hilbert (EH) action, as the latter derived it when working on a theory combining GR and electromagnetism.

As mentioned in the introduction, GR is incomplete at high energies. It is for this reason, among others, that theoreticians have been proposing corrections to this EH action. Over time, correcting this action evolved into what is now known as Modified Gravity. Currently, there exists an extensive amount of MG theories. Ref. [13] groups them into four gravity classes:

- Tensor-Vector-Scalar (TeVeS) Gravity, which consists of adding Tensor, Vector, or Scalar fields to the EH action.
- Higher-Derivative Gravity, which consists of adding curvature invariants that contain more derivatives than the Ricci scalar in the EH action.
- Non-Riemannian Gravity, in which the geometrical foundations of GR are modified.
- Quantum Theories of Gravity, where modifications follow from quantum mechanics. Note that while the previous categories focus on classical gravity, the theories in this class are meant to treat scenarios where both gravitational and quantum-mechanical effects are significant.

Ref. [6] studies some properties of a rotating black hole at its ergosphere and horizon. Here, GR is modified with a natural generalization of Higher-Derivative Gravity, where the Ricci tensor from the EH action, and all the curvature invariants of six derivatives, are arranged in an Effective Field Theory fashion. This thesis extends the mentioned generalization by including the curvature invariants of eight derivatives presented in Ref. [10]. Thus, before deriving or obtaining any results, it was necessary to understand the actions Refs.[6, 10] propose. The following subsection 2.1 gives a brief overview of EFT, which will allow a better understanding of subsection 2.2, where the mentioned proposed actions, as well as the action used in this thesis, are introduced.

2.1 Overview of Effective Field Theory

EFT is a method for constructing an approximation that focuses on a subrange of the energy scale of an underlying theory. One consequence of this selection is that observables are calculated more easily as compared to using the complete theory. These concepts are captured by the general scheme any EFT Lagrangian follows:

$$\mathcal{L}_{\text{EFT}} = \sum_{\mathcal{D}\geq 0,i} \frac{c_i^{(\mathcal{D})}\mathcal{O}_i^{(\mathcal{D})}}{\Lambda^{\mathcal{D}-d}}\,. \tag{2.2}$$

EFT assumes natural units, where the speed of light c and the reduced Plank constant $\hbar$ are set to one. This implies that all quantities have the unit of energy raised to some power. In this context, the mass dimension[3], or simply the dimension of a quantity, is precisely this power. Turning to this EFT scheme, its operators $\mathcal{O}_i^{(\mathcal{D})}$ have dimension $\mathcal{D}$, $[\mathcal{O}_i^{(\mathcal{D})}] = \mathcal{D}$, and agree with the symmetries of the complete theory. The energy limit Λ, is the maximum energy at which the phenomena of interest can occur, and in practice, it is the maximum energy at which the effective action leads to correct observables. It is introduced so that the coefficients $c_i^{(\mathcal{D})}$ are dimensionless, and because it is an energy, $[\Lambda] = 1$. The exponent $\mathcal{D} - d$ follows from the fact that any action is dimensionless in natural units. This implies that in d spacetime dimensions, the corresponding Lagrangian has dimension d. Thus, with operators of dimension $\mathcal{D}$ multiplied by dimensionless coefficients, the Λ exponent with which the EFT Lagrangian has dimension d is $\mathcal{D} - d$. The quotients $c_i^{(\mathcal{D})}/\Lambda^{\mathcal{D}-d}$ often appear in EFT observables, and in many sources, they are referred to as Wilson coefficients. This sum is truncated at a $\mathcal{D}$ with which the factor $1/\Lambda^{\mathcal{D}-d}$ is negligible, and this limit depends on the underlying theory and the energies of the phenomena of interest. Finally, this scheme implies that as the operators' dimension increases, so does the suppression from their corresponding Wilson coefficient. Hence, i) EFT can only be applied to theories where the operators with higher dimension are, or can be, associated with energies that are closer to the upper limit of the energy range of interest. ii) The operators, along with their dimensionless coefficients, must be sufficiently large to get to modify the EH action despite this $1/\Lambda^{\mathcal{D}-d}$ suppression.

2.2 Higher-Derivative Gravity as an Effective Field Theory

As mentioned in the introduction, the operators of an EFT of gravity are combinations of curvature tensors that agree with the symmetries of GR: invariance under arbitrary differentiable coordinate transformations, also called general covariance. This symmetry only allows curvature invariants, that is, operators consisting of scalar combinations of R, R_{ab}, and $R_{ab\alpha\beta}$, and their covariant derivatives. In GR, the dimension of the operators is given by the number of partial derivatives in each of their terms [6]. For example, when expanding the Christoffel symbols in the definition of the Riemann tensor, one can see that

[3] $E = m$, thus, a mass dimension is an energy dimension.

the resulting terms have two derivatives each. Therefore, $[R_{abcd}] = [R_{ab}] = [R] = 2$, with natural units implying that $[\partial] = 1$. Classifying the curvature invariants by their number of derivatives seems therefore practical.

Appendix A of Ref. [6] starts the derivation of its general Higher-Derivative action by considering the following parametrization

$$S \equiv \frac{1}{16\pi G}\int d^4x\sqrt{-g}R + \sum_{n\geq 2}\frac{\ell^{2n-2}}{16\pi G}S^{(2n)} \tag{2.3}$$

where $2n$ indicates the number of derivatives, ℓ is the characteristic length scale of the horizon and ergosphere spacetime, and the four-dimensional action $S^{(2n)}$ contains a sum of curvature invariants of dimension $2n$ multiplied by coupling constants. Three observations can be made: i) Since energy and length are inversely proportional, $[E] = 1/[L]$, ℓ is equivalent to the limit $1/\Lambda^{\mathcal{D}-d}$ in 2.2, ii) With G of dimension two, the coupling constants in $S^{(2n)}$ are equivalent to $c_i^{(\mathcal{D})}$ in 2.2. iii) Due to the exponents $2n-2$, and in the regime of validity, invariants with more derivatives get more suppressed, in agreement with the EFT philosophy. The derivation finishes with the determination of all independent curvature invariants from $2n = 2$ to $2n = 6$, discarding operators when necessary. It is important to clarify that the reference, [6], relaxes the general covariance restriction to admit operators that are not invariant under parity transformations, at which all the spacial coordinates flip their sign. This means that scalar combinations containing dual curvature tensors and their covariant derivatives are also considered. Starting with two derivatives, the only possibility is R, which is already in the EH action. It is well-known that the corresponding EOM is the Einstein tensor equated to zero. Here, it follows that R_{ab} and R vanish, so operators written in terms of these tensors can be discarded (see beginning of section 4.1). Continuing with four derivatives, $S^{(4)}$ reads

$$S^{(4)} = \int d^4x\sqrt{-g}\left(\alpha_1\mathcal{X}_4 + \alpha_2 R_{abcd}\tilde{R}^{abcd} + \alpha_3 R_{ab}R^{ab} + \alpha_4 R^2\right). \tag{2.4}$$

Both $\sqrt{-g}\mathcal{X}_4$[4] and $\sqrt{-g}R_{abcd}\tilde{R}^{abcd}$ can be written as a total derivative of a field [6]. By Stoke's theorem, their integrals over the spacetime volume vanish, so these terms do not contribute to the EOM. Regarding $\alpha_3 R_{ab}R^{ab}$ and $\alpha_4 R^2$, they can be discarded by the discussion in the two-derivative part. In contrast, none of the independent six-derivative operators should be discarded, as they cannot be written in terms of total derivatives nor in terms of the Ricci tensor or the Ricci scalar. Thus, the Higher-Derivative generalization Ref.[6] proposes reads

$$S = \frac{1}{16\pi G}\int d^4x\sqrt{-g}\left(R + \lambda_{\rm ev}\ell^4 R_{ab}{}^{cd}R_{cd}{}^{ef}R_{ef}{}^{ab} + \lambda_{\rm odd}\ell^4 R_{ab}{}^{cd}R_{cd}{}^{ef}\tilde{R}_{ef}{}^{ab}\right), \tag{2.5}$$

[4] $\mathcal{X}_4$ is known as the four-dimensional Euler Density or Gauss-Bonnet term. Ref [14] shows how to express $\sqrt{-g}\mathcal{X}_4$ as a total derivative.

where operators associated with the couplings $\lambda_{\rm ev}$ and $\lambda_{\rm odd}$ are invariant and variant under a parity transformation, respectively. As the labels suggest, one can also refer to this behavior as even or odd.

In Ref. [10], the (independent) eight-derivative corrections are considered. However, the six-derivative ones are discarded for reasons in Ref. [15] that nowadays are known to be incorrect.

With all this in mind, the action of this thesis, also the one used in [12], reads

$$\begin{aligned} S &= \frac{1}{16\pi G}\int d^4x\sqrt{-g}\left(R+\ell^4\mathcal{L}_{(6)}+\ell^6\mathcal{L}_{(8)}\right)\,,\\ \mathcal{L}_{(6)} &= \lambda_{\rm ev}R_{ab}{}^{cd}R_{cd}{}^{ef}R_{ef}{}^{ab}+\lambda_{\rm odd}R_{ab}{}^{cd}R_{cd}{}^{ef}\tilde{R}_{ef}{}^{ab}\,,\\ \mathcal{L}_{(8)} &= \epsilon_1\mathcal{C}^2+\epsilon_2\tilde{\mathcal{C}}^2+\epsilon_3\mathcal{C}\tilde{\mathcal{C}}\,,\\ &\text{with}\\ \mathcal{C} &= R_{abcd}R^{abcd}\,,\quad \tilde{\mathcal{C}}=R_{abcd}\tilde{R}^{abcd}\,,\quad \tilde{R}^{abcd}=\frac{1}{2}\epsilon^{abef}R_{ef}{}^{cd}\,. \end{aligned} \tag{2.6}$$

where the operators associated with ϵ_1 and ϵ_2 are parity-even, while the operator associated with ϵ_3 is parity-odd. For brevity, any result that comes from, or is related to, these six or eight-derivative action corrections, will also hold the adjective six-derivative or eight-derivative as applicable. For example, the eight-derivative correction to the angular velocity at the horizon does not contain eight derivatives, but comes from the eight-derivative curvature invariants of this thesis action.

3 Reproducing the equations of motion

3.1 Deriving the Euler-Lagrange Equations

Most textbooks and articles derive Euler-Lagrange (EL) equations for Lagrangians that depend on a field and its first partial derivative. However, the expansion of the curvature invariants considered in this thesis reveals an additional dependence on the second partial derivative of the metric field. It was necessary then to generalize the EL equations. They were derived from first principles, as shown below.

First, the Principle of Least Action is applied:

$$S\left[g_{ab}\right]=\int_\Omega \mathcal{L}\left(g_{ab},\partial_c g_{ab},\partial_c\partial_d g_{ab}\right)d\Omega \tag{3.7}$$

$$\Rightarrow \delta S=\int_\Omega\left(\frac{\delta\mathcal{L}}{\delta g_{ab}}\delta g_{ab}+\frac{\delta\mathcal{L}}{\delta\partial_c g_{ab}}\delta\partial_c g_{ab}+\frac{\delta\mathcal{L}}{\delta\partial_c\partial_d g_{ab}}\delta\partial_c\partial_d g_{ab}\right)d\Omega=0\,. \tag{3.8}$$

It is convenient to rewrite this condition such that the variation of the metric, δg_{ab}, becomes a common factor to all three terms.
Starting with the second term of the integrand, by using the commutation of a variation and a partial derivative,

$$\delta\partial_c g_{ab} = \partial_c \delta g_{ab}\,, \tag{3.9}$$

it is possible to express it as a dot product between a vector field $\bar{F}$ and the divergence of g

$$\frac{\delta\mathcal{L}}{\delta\partial_c g_{ab}}\delta\partial_c g_{ab} \Leftrightarrow \underbrace{\left(\frac{\delta\mathcal{L}}{\delta\partial_0 g_{ab}},\ldots,\frac{\delta\mathcal{L}}{\delta\partial_3 g_{ab}}\right)}_{\bar{F}} \cdot \underbrace{\left((\partial_0,\ldots,\partial_3)\,\delta g_{ab}\right)}_{\bar{\nabla} g}\,. \tag{3.10}$$

The integral can then be rewritten using integration by parts

$$\begin{aligned} &\Rightarrow \int_\Omega \frac{\delta\mathcal{L}}{\delta\partial_c g_{ab}}\delta\partial_c g_{ab}\,d\Omega = \int_\Omega \bar{F}\cdot\bar{\nabla} g\,d\Omega = \\ &= \cancelto{0}{\int_{\partial\Omega} g\bar{F}\cdot\hat{n}\,d\Omega} - \int_\Omega g\bar{\nabla}\cdot\bar{F}d\Omega = -\int_\Omega \delta g_{ab}\,\partial_c\frac{\delta\mathcal{L}}{\delta\partial_c g_{ab}}\,d\Omega\,, \end{aligned} \tag{3.11}$$

where the surface integral does not contribute since fields are assumed to be zero at infinity.

Considering the third term in the integrand, Eq. (3.8), first, the chain rule is applied:

$$\frac{\delta\mathcal{L}}{\delta\partial_c\partial_d g_{ab}}\partial_c\partial_d\delta g_{ab} = \partial_c\left[\frac{\delta\mathcal{L}}{\delta\partial_c\partial_d g_{ab}}\partial_d\delta g_{ab}\right] - \left[\left(\partial_c\frac{\delta\mathcal{L}}{\delta\partial_c\partial_d g_{ab}}\right)(\partial_d\delta g_{ab})\right]\,. \tag{3.12}$$

The first resulting term can be rewritten as the divergence of a vector field $\bar{F}'$, so its integral can then be solved by applying Gauss' Theorem:

$$\partial_c\left[\frac{\delta\mathcal{L}}{\delta\partial_c\partial_d g_{ab}}\partial_d\delta g_{ab}\right] \Leftrightarrow \underbrace{(\partial_0,\ldots,\partial_3)}_{\bar{\nabla}}\cdot\underbrace{\left(\frac{\delta\mathcal{L}}{\delta\partial_{0d} g_{ab}}\partial_d\delta g_{ab},\ldots,\frac{\delta\mathcal{L}}{\delta\partial_{3d} g_{ab}}\partial_d\delta g_{ab}\right)}_{\bar{F}'} \tag{3.13}$$

$$\Rightarrow \int_\Omega \partial_c\left[\frac{\delta\mathcal{L}}{\delta\partial_c\partial_d g_{ab}}\partial_d\delta g_{ab}\right]d\Omega = \int_\Omega \bar{\nabla}\cdot\bar{F}'d\Omega = \int_{\partial\Omega}\bar{F}'\cdot d\overline{\partial\Omega} = 0\,, \tag{3.14}$$

The second resulting term can be expressed as dot products between vector fields $\bar{F}_{c=0}$ ...

$\bar{F}_{c=3}$ and the divergence of the same g, as in Eq. (3.10), yielding

$$\begin{aligned} &- \left(\partial_c \frac{\delta \mathcal{L}}{\delta \partial_c \partial_d g_{ab}}\right)(\partial_d \delta g_{ab}) = \\ &= - \left(\partial_0 \frac{\delta \mathcal{L}}{\delta \partial_0 \partial_d g_{ab}}\right)(\partial_d \delta g_{ab}) - \cdots - \left(\partial_3 \frac{\delta \mathcal{L}}{\delta \partial_3 \partial_d g_{ab}}\right)(\partial_d \delta g_{ab}) \end{aligned} \tag{3.15}$$

$$\left(\partial_0 \frac{\delta \mathcal{L}}{\delta \partial_0 \partial_d g_{ab}}\right)(\partial_d \delta g_{ab}) \Leftrightarrow \underbrace{\left(\partial_0 \frac{\delta \mathcal{L}}{\delta \partial_0 \partial_0 g_{ab}}, \ldots, \partial_0 \frac{\delta \mathcal{L}}{\delta \partial_0 \partial_3 g_{ab}}\right)}_{\bar{F}_{c=0}} \cdot \underbrace{((\partial_0, \ldots, \partial_3)\, \delta g_{ab})}_{\bar{\nabla} g} . \tag{3.16}$$

The integral can then be rewritten using integration by parts as

$$\Rightarrow \int_\Omega -\bar{F}_{c=0} \cdot \bar{\nabla} g = \int_\Omega g \bar{\nabla} \cdot \bar{F}_{c=0}\, d\Omega = \int_\Omega \delta g_{ab} \left(\partial_d \partial_0 \frac{\delta \mathcal{L}}{\delta \partial_0 \partial_d g_{ab}}\right) d\Omega \tag{3.17}$$

$$\Rightarrow \int_\Omega - \left(\partial_c \frac{\delta \mathcal{L}}{\delta \partial_c \partial_d g_{ab}}\right)(\partial_d \delta g_{ab})\, d\Omega = \int_\Omega \delta g_{ab} \left(\partial_c \partial_d \frac{\delta \mathcal{L}}{\delta \partial_c \partial_d g_{ab}}\right) d\Omega\,. \tag{3.18}$$

With the variation Eq. (3.8) rewritten according to Eq. (3.11) and Eq. (3.18), the EL equations can finally be determined:

$$\delta S = \int_\Omega \left(\frac{\delta \mathcal{L}}{\delta g_{ab}} - \partial_c \frac{\delta \mathcal{L}}{\delta \partial_c g_{ab}} + \partial_c \partial_d \frac{\delta \mathcal{L}}{\delta \partial_c \partial_d g_{ab}}\right) \delta g_{ab} = 0 \tag{3.19}$$

$$\Rightarrow \frac{\delta \mathcal{L}}{\delta g_{ab}} - \partial_c \frac{\delta \mathcal{L}}{\delta \partial_c g_{ab}} + \partial_c \partial_d \frac{\delta \mathcal{L}}{\delta \partial_c \partial_d g_{ab}} = 0 \quad (\forall \delta g_{ab})\,. \tag{3.20}$$

3.2 Applying the Euler-Lagrange Equations

With the suitable EL equations, the derivation of the EOM associated with this thesis action was then possible.

Starting with the application of these EL equations to the EH action, it is well-known that the result is the Einstein tensor equated to zero. In Refs. [6, 10, 12], the EL equations are applied to the action corrections so that the result can be considered as an effective energy-momentum tensor. The word effective is significant because those references, and this thesis, are interested in a vacuum solution. Following this scheme, the EOM of this thesis then read

$$G_{ab} = T^{\text{eff}}_{ab} \quad \Leftrightarrow \quad R_{ab} - \frac{1}{2} g_{ab} R = \ell^4\, T^{\text{eff}\,(6)}_{ab} + \ell^6\, T^{\text{eff}\,(8)}_{ab}\,, \tag{3.21}$$

with

$$\ell^4 T_{ab}^{\text{eff}\,(6)} = \lambda_{\text{ev}}\ell^4 \left[3R_a{}^{cde} R_{de}{}^{fg} R_{fgcb} + \frac{1}{2} g_{ab} R_{cd}{}^{ef} R_{ef}{}^{gh} R_{gh}{}^{cd} - 6\nabla^c \nabla^d \left(R_{acef} R_{bd}{}^{ef} \right) \right]$$
$$+ \lambda_{\text{odd}}\ell^4 \Bigg[- \frac{3}{2} R_a{}^{cde} R_{defg} \tilde{R}_{bc}{}^{fg} - \frac{3}{2} R_a{}^{cde} R_{bcfg} \tilde{R}_{de}{}^{fg} + \frac{1}{2} g_{ab} R_{cd}{}^{ef} R_{ef}{}^{gh} \tilde{R}_{gh}{}^{cd} \tag{3.22}$$
$$+ 3\nabla^c \nabla^d \left(R_{acef} \tilde{R}_{bd}{}^{ef} + R_{bdef} \tilde{R}_{ac}{}^{ef} \right) \Bigg] ,$$

and

$$\ell^6 T_{ab}^{\text{eff}\,(8)} = \epsilon_1 \ell^6 \left(8R_{acbd} \nabla^c \nabla^d \mathcal{C} + \frac{1}{2} g_{ab} \mathcal{C}^2 \right) + \epsilon_2 \ell^6 \left(8\tilde{R}_{acbd} \nabla^c \nabla^d \tilde{\mathcal{C}} + \frac{1}{2} g_{ab} \tilde{\mathcal{C}}^2 \right)$$
$$+ \epsilon_3 \ell^6 \left(4\tilde{R}_{acbd} \nabla^c \nabla^d \mathcal{C} + 4R_{acbd} \nabla^c \nabla^d \tilde{\mathcal{C}} + \frac{1}{2} g_{ab} \tilde{\mathcal{C}} \mathcal{C} \right) , \tag{3.23}$$

where Eqs. (3.22) and (3.23) are reproductions of Eqs. (2.13) and (2) in [6] and [10], respectively.

These reproductions were mostly achieved analytically with the packages xTensor[16] and xTras[17], with a few steps performed numerically with the package xCoba[18]. The EL equations of this thesis were applied via the command `VarL[ ]` from xTras. The results were always lengthy expansions of up to thirty-four terms. To reduce them to their final forms written above, a vanishing Ricci tensor was first assumed[5], as specified in [10], and afterwards, certain properties that derive from this assumption were applied via Mathematica's replacement rules. Those properties can be deduced as follows:

i) The Weyl Tensor of $n > 2$ spacetime dimensions

$$C_{iklm} = R_{iklm} + \frac{1}{n-2} \left(R_{im} g_{kl} - R_{il} g_{km} + R_{kl} g_{im} - R_{km} g_{il} \right) +$$
$$+ \frac{1}{(n-1)(n-2)} R \left(g_{il} g_{km} - g_{im} g_{kl} \right) , \tag{3.24}$$

equals then the Riemann tensor. This, in turn, means that the Weyl identities from Refs. [19, 20] (Eq. 3.18 in Ref. [20]) can be written as

$$R_{ebcd} R_f{}^{bcd} = \frac{1}{4} g_{ef} R_{abcd} R^{abcd} , \tag{3.25}$$

$$\tilde{R}_{ebcd} R_f{}^{bcd} = \frac{1}{4} g_{ef} \tilde{R}_{abcd} R^{abcd} . \tag{3.26}$$

[5] This assumption is justified later in subsection 4.1

ii) The Riemann and Dual Riemann tensors have the same symmetries [21].
iii) The contraction of the Bianchi identity

$$g^{ml}\left(\nabla_l R_{abmn} + \nabla_n R_{ablm} + \nabla_m R_{abnl}\right) = 0 \quad \Leftrightarrow \quad 2\nabla^m R_{abmn} + \cancelto{0}{\nabla_n R_{ab\ m}^{\ m}} = 0 \tag{3.27}$$

implies that

$$\nabla^m R_{abmn} = 0\,. \tag{3.28}$$

Because of length constraints, the reproduction of the EOM Eqs. (3.22) and (3.23) cannot be shown in full detail. However, the reproduction of the part $4\tilde{R}_{acbd}\nabla^c\nabla^d\mathcal{C}+4R_{acbd}\nabla^c\nabla^d\tilde{\mathcal{C}}+\frac{1}{2}g_{ab}\tilde{\mathcal{C}}\mathcal{C}$ from the EOM Eq. (3.23) is sketched in appendix A. It is a representative derivation since all the above properties were applied. The remaining terms were derived similarly.

4 Solving the equations of motion

The next task after reproducing the EOM from Refs. [6] and [10] was to solve for the metric. By introducing corrections to the EH action, the Kerr metric no longer solves the resulting gravitational field equations for the case of a rotating black hole[6]. One would think then that solving the EOM of this thesis is a challenging task. However, note that these equations come from corrections that are small around the event horizon of a rotating black hole [6][7]. Thus, the solution was assumed to be similar to the Kerr metric, which allowed for the use of perturbation theory. In section 4.1, perturbation theory will be applied to the EOM, which will be used in section 4.2 after motivating the ansatz to be inserted in the perturbed EOM.

4.1 Perturbing the equations of motion

In gravity, perturbation theory relies on assuming a family of manifolds equipped with a metric field, such that those manifolds, their metrics, and any other tensor fields on them depend on a dimensionless parameter ε. This parametrization must be done such that $\varepsilon = 0$ refers to the tensors of the exact solution, also called background members [22]. In this thesis, those members are a 4-dimensional manifold with the Kerr metric, the Einstein tensor according to such metric, and a vanishing Energy-Momentum tensor. Since all corrections are small, tensor fields can be approximated by Taylor expanding around $\varepsilon = 0$. Any tensor in the family then reads

$$A_{ab}(\varepsilon) = A_{ab}(0) + \varepsilon\frac{dA_{ab}}{d\varepsilon}\Big|_{\varepsilon=0} + \frac{1}{2}\varepsilon^2\frac{d^2A_{ab}}{d\varepsilon^2}\Big|_{\varepsilon=0} + \cdots := A^{(0)}_{ab} + A^{(1)}_{ab} + A^{(2)}_{ab} + \cdots\,. \tag{4.29}$$

[6]More generally, Ricci flat metrics do not solve the gravitational field equations from Higher-Derivative theories [6].

[7]Corrections are small when $M >> \ell$, and this is the case of the horizon and ergosphere.

Note that all the terms are evaluated at $\varepsilon = 0$, meaning that they are computed using the well-known background metric. This is the reason that the EOM of this thesis were derived assuming $R_{ab} = 0$ (see properties of the Kerr metric in section 4.2).

Following [6, 12], the effective Energy-Momentum Tensor, Eq. (3.21), can be treated as a first-order perturbation. Then, taking into account that the background Energy-Momentum Tensor is null, and using the notation in Eq. (4.29), the following holds

$$G_{ab} = T_{ab} \tag{4.30}$$

$$G^{(0)}_{ab} + G^{(1)}_{ab} = \cancelto{0}{T^{(0)}_{ab}} + T^{(1)}_{ab} \tag{4.31}$$

$$G^{(0)}_{ab} = 0 \tag{4.32}$$

$$G^{(1)}_{ab} = T^{(1)}_{ab} \quad \Leftrightarrow \quad \underbrace{G_{ab} - G^{(0)}_{ab}}_{\delta G_{ab}} = T^{\text{eff}}_{ab}\,, \tag{4.33}$$

so the metric ansatz to consider is

$$g_{ab} = g^{(0)}_{ab} + \underbrace{\ell^4 g^{(6)}_{ab} + \ell^6 g^{(8)}_{ab}}_{g^{(1)}_{ab}}, \tag{4.34}$$

where $\ell^4 g^{(6)}_{ab}$ and $\ell^6 g^{(8)}_{ab}$ are metric corrections that account for the six and eight-derivative action corrections, respectively.

Hence, the EOM of this thesis are perturbed by inserting the metric expansion Eq. (4.34) into the perturbation, δG_{ab}, in Eq. (4.33), discarding the resulting negligible terms ($\mathcal{O}(l^8)$, or $\mathcal{O}(\varepsilon^2)$) where applicable and evaluating at the Kerr metric. As will be seen below, the result will be two decoupled differential equations that allow to solve for the metric corrections.

Ref. [23] derives the first-order perturbation of the Einstein tensor corresponding to a general curved vacuum spacetime. Based on the notation this reference uses, and for convenience, any background member will have the superscript B, $g^{(1)}_{ab}$ will be substituted by h_{ab} and therefore $l^4 g^{(6)}_{ab}$ and $l^6 g^{(8)}_{ab}$ will be denoted by $h^{(6)}_{ab}$ and $h^{(8)}_{ab}$, respectively. For completeness, such derivation is included in appendix B. To reduce computational time when solving the EOM, this expression was rewritten *only* in terms of the background covariant derivative and the traced-reverse metric perturbation $\bar{h}_{bd} = h_{bd} - \frac{1}{2} g^{\mathrm{B}}_{bd} g^{\mathrm{B}\,ac} h_{ac}$. This adaptation was carried on in the following way:

Starting with the perturbed Einstein tensor from [23]

$$\delta G_{bd} = -\frac{1}{2}\Box^{\mathrm{B}} \bar{h}_{bd} + R^{\mathrm{B}}_{adbc} \bar{h}^{ac} - \frac{1}{2} g^{\mathrm{B}}_{bd} \nabla^{\mathrm{B}}_a \nabla^{\mathrm{B}}_c \bar{h}^{ac} + \frac{1}{2} \nabla^{\mathrm{B}}_b \nabla^{\mathrm{B}}_a \bar{h}^{a}{}_{d} + \frac{1}{2} \nabla^{\mathrm{B}}_d \nabla^{\mathrm{B}}_a \bar{h}^{a}{}_{b}\,, \tag{4.35}$$

the term with the Riemann tensor can be removed by first applying the commutation of covariant derivatives in GR, $[\nabla^{\mathrm{B}}_a, \nabla^{\mathrm{B}}_b] T_{cd} = -R^{\mathrm{B}\,e}{}_{cab} T_{ed} - R^{\mathrm{B}\,e}{}_{dab} T_{ce}$ [24], on the last two

terms, yielding

$$\nabla^{\mathrm{B}}_b\nabla^{\mathrm{B}}_a\bar{h}^a{}_d = \nabla^{\mathrm{B}}_a\nabla^{\mathrm{B}}_b\bar{h}^a{}_d - R^{\mathrm{B}a}{}_{e}{}^{ba}\bar{h}^e{}_d - R^{\mathrm{B}}{}_{e}{}^{dba}\bar{h}^a{}_e \tag{4.36}$$

$$\nabla^{\mathrm{B}}_d\nabla^{\mathrm{B}}_a\bar{h}^a{}_b = \nabla^{\mathrm{B}}_a\nabla^{\mathrm{B}}_d\bar{h}^a{}_b - R^{\mathrm{B}}{}_{e}{}^{bda}\bar{h}^a{}_e\,, \tag{4.37}$$

and then, applying the symmetries of the Riemann tensor to the previous result along with the second term

$$\begin{aligned} &R^{\mathrm{B}}_{adbc}\bar{h}^{ac} + \frac{1}{2}\nabla^{\mathrm{B}}_b\nabla^{\mathrm{B}}_a\bar{h}^a{}_d + \frac{1}{2}\nabla^{\mathrm{B}}_d\nabla^{\mathrm{B}}_a\bar{h}^a{}_b = \\ &= R^{\mathrm{B}}_{adbc}\bar{h}^{ac} + \frac{1}{2}\nabla^{\mathrm{B}}_a\nabla^{\mathrm{B}}_b\bar{h}^a{}_d - \frac{1}{2}R^{\mathrm{B}\,c}{}_{dba}\bar{h}^a{}_c + \frac{1}{2}\nabla^{\mathrm{B}}_a\nabla^{\mathrm{B}}_d\bar{h}^a{}_b - \frac{1}{2}R^{\mathrm{B}\,c}{}_{bda}\bar{h}^a{}_c = \\ &= \frac{1}{2}\nabla^{\mathrm{B}}_a\nabla^{\mathrm{B}}_b\bar{h}^a{}_d + \frac{1}{2}\nabla^{\mathrm{B}}_a\nabla^{\mathrm{B}}_d\bar{h}^a{}_b\,. \end{aligned} \tag{4.38}$$

Then the first-order perturbation of the Einstein tensor in terms of the background covariant derivative and the trace-reversed metric perturbation reads

$$\delta G_{bd} = -\frac{1}{2}\Box^{\mathrm{B}}\bar{h}_{bd} - \frac{1}{2}g^{\mathrm{B}}_{bd}\nabla^{\mathrm{B}}_a\nabla^{\mathrm{B}}_c\bar{h}^{ac} + \frac{1}{2}\nabla^{\mathrm{B}}_a\nabla^{\mathrm{B}}_b\bar{h}^a{}_d + \frac{1}{2}\nabla^{\mathrm{B}}_a\nabla^{\mathrm{B}}_d\bar{h}^a{}_b\,, \tag{4.39}$$

from which the perturbed Einstein tensor (2.15) in Ref. [6] can be recovered by only including the six-derivative metric correction $h^{(6)}_{ab}$ in the trace-reversed metric perturbation.

With both sides of Eq. (4.30) properly perturbed, by first expanding the trace-reversed metric perturbation

$$\begin{aligned} \bar{h}_{ab} &= \left(h^{(6)}_{ab} + h^{(8)}_{ab}\right) - \frac{1}{2}g^{\mathrm{B}}_{ab}g^{\mathrm{B}\,cd}\left(h^{(6)}_{cd} + h^{(8)}_{cd}\right) = \\ &= \left(h^{(6)}_{ab} - \frac{1}{2}g^{\mathrm{B}}_{ab}g^{\mathrm{B}\,cd}h^{(6)}_{cd}\right) + \left(h^{(8)}_{ab} - \frac{1}{2}g^{\mathrm{B}}_{ab}g^{\mathrm{B}\,cd}h^{(8)}_{cd}\right) := \bar{h}^{(6)}_{ab} + \bar{h}^{(8)}_{ab}\,, \end{aligned} \tag{4.40}$$

plugging this expansion into the LHS, and then gathering the resulting terms by order in ℓ, the perturbed EOM of this thesis are obtained

$$-\frac{1}{2}\Box^{\mathrm{B}}\bar{h}_{bd} - \frac{1}{2}g^{\mathrm{B}}_{bd}\nabla^{\mathrm{B}}_a\nabla^{\mathrm{B}}_c\bar{h}^{ac} + \frac{1}{2}\nabla^{\mathrm{B}}_a\nabla^{\mathrm{B}}_b\bar{h}^a{}_d + \frac{1}{2}\nabla^{\mathrm{B}}_a\nabla^{\mathrm{B}}_d\bar{h}^a{}_b = T^{\mathrm{eff}}_{bd} \tag{4.41}$$

$$\Rightarrow -\frac{1}{2}\Box^{\mathrm{B}}\bar{h}^{(6)}_{bd} - \frac{1}{2}g^{\mathrm{B}}_{bd}\nabla^{\mathrm{B}}_a\nabla^{\mathrm{B}}_c\bar{h}^{(6)\,ac} + \frac{1}{2}\nabla^{\mathrm{B}}_a\nabla^{\mathrm{B}}_b\bar{h}^{(6)\,a}{}_d + \frac{1}{2}\nabla^{\mathrm{B}}_a\nabla^{\mathrm{B}}_d\bar{h}^{(6)\,a}{}_b = \ell^4\,T^{\mathrm{eff}\,(6)}_{bd} \tag{4.42}$$

$$\Rightarrow -\frac{1}{2}\Box^{\mathrm{B}}\bar{h}^{(6)}_{bd} - \frac{1}{2}g^{\mathrm{B}}_{bd}\nabla^{\mathrm{B}}_a\nabla^{\mathrm{B}}_c\bar{h}^{(8)\,ac} + \frac{1}{2}\nabla^{\mathrm{B}}_a\nabla^{\mathrm{B}}_b\bar{h}^{(8)\,a}{}_d + \frac{1}{2}\nabla^{\mathrm{B}}_a\nabla^{\mathrm{B}}_d\bar{h}^{(8)\,a}{}_b = \ell^6\,T^{\mathrm{eff}\,(8)}_{bd} \tag{4.43}$$

4.2 Correcting the Kerr metric

The ansatz of the metric corrections to this thesis is based on Ref. [6]. In this reference, the authors start the construction of a four-derivative metric correction by reviewing the

Kerr metric. Some properties of this metric, along with previous works, motivate the correction they propose. This subsection outlines this process[8], from which later on an eight-derivative metric correction is deduced.

Kerr's metric in Boyer-Lindquist coordinates reads:

$$\begin{aligned} ds^2 = &- \left(1 - \frac{2Mr}{\Sigma}\right) dt^2 - \frac{4Mar\sin^2\theta}{\Sigma} dt d\phi + \Sigma \left(\frac{dr^2}{\Delta} + d\theta^2\right) \\ &+ \left(r^2 + a^2 + \frac{2Mra^2\sin^2\theta}{\Sigma}\right) \sin^2\theta d\phi^2 \end{aligned} \tag{4.44}$$

where

$$\Sigma = r^2 + a^2\cos^2\theta\,, \quad \Delta = r^2 - 2Mr + a^2\,. \tag{4.45}$$

Some of the properties of this metric are

- It is a solution of vacuum Einstein's Field Equations (EFE), so it is Ricci flat $R_{ab} = 0$.
- It represents a spacetime with total mass M and angular momentum $J = aM$. The parameter a is the angular momentum per mass, and its sign indicates the direction of rotation.
- It is stationary and axisymmetric around the axis of rotation. Equivalently, its Killing vectors are the basis vectors ∂_t and ∂_ϕ (see discussion below 5.58).
- It is asymptotically flat.
- Its inner $(-)$ and outer $(+)$ horizons are placed at the roots of $\Delta = 0$:

  $$r_\pm = M \pm \sqrt{M^2 - a^2}\,, \tag{4.46}$$

  so those horizons exist as long as

  $$-M \leq a \leq M\,, \tag{4.47}$$

The authors expect the metric correction to maintain these properties except for the Ricci flatness. Additionally, they also expect it to not activate the vanishing components of the Kerr metric. With these conditions in mind, the authors propose the following general correction

$$\begin{aligned} g^{(6)}_{\mu\nu} dx^\mu dx^\nu = &\, H_1 dt^2 - H_2 \frac{4Ma\rho(1-x^2)}{\Sigma} dt d\phi + H_3 \Sigma \left(\frac{d\rho^2}{\Delta} + \frac{dx^2}{1-x^2}\right) \\ &+ H_4 \left(\rho^2 + a^2 + \frac{2M\rho a^2(1-x^2)}{\Sigma}\right)(1-x^2) d\phi^2 \end{aligned} \tag{4.48}$$

[8] the detailed derivation is in section 3 in Ref. [6].

where

$$\Sigma = \rho^2 + a^2 x^2 \,, \quad \Delta = \rho^2 - 2M\rho + a^2 \,. \tag{4.49}$$

The functions $H_{1,2,3,4}$ depend on $x = \cos\theta$ and ρ. They are asummed to be small, $|H_i| << 1$, and they behave asymptotically as

$$H_i = h_i^{(0)} + \frac{h_i^{(1)}}{\rho} + \mathcal{O}\left(\frac{1}{\rho^2}\right) \,, \; i = 1, 2, 3, 4 \,, \tag{4.50}$$

where the following values for the constant coefficients $h_i^{(k)}$ make the correction asymptotically flat

$$h_1^{(0)} = 0 \,, \quad h_3^{(0)} = h_4^{(0)} = -\frac{h_3^{(1)}}{M} \,, \quad h_2^{(0)} = -\frac{h_3^{(0)}}{2} \,. \tag{4.51}$$

It is important to mention that actually, the most general four-derivative metric correction contains five H_i functions. However, thanks to the freedom of choice of coordinates, the authors performed an infinitesimal coordinate trasnformation $(x, \rho) \to (x', \rho')$ that preserves the form of the whole metric and for which $H_5' = H_3'$. The authors then chose $H_5 = H_3$, which lead to the more convenient correction Eq. (4.48).

The horizons are still given by $\Delta = 0$, with the solution $\rho_\pm$ indicating their location. Consequently, the condition Eq. (4.47) applies as well.

If the authors of [6] had plugged the correction Eq. (4.48) in their perturbed EOM ((2.13) and (2.17) in [6], or Eq. (4.42) in this thesis, the resulting system of equations, with the functions H_i as the unknowns, would have been difficult to solve. Based on numerous works, the authors refine their initial proposal by expanding H_i in the following way:

The spin, or angular momentum per mass squared, is introduced

$$\chi = \frac{a}{M} \,. \tag{4.52}$$

From Eq. (4.47) one can deduce that $\chi \in [-1, 1]$. Hence, if the mass takes its minimum possible value, $\chi = \pm 1$, this is referred to as an "extremal black hole".
Then the authors express H_i functions as a power series in χ:

$$H_i = \sum_{n=0}^{\infty} H_i^{(n)} \chi^n \,, \quad H_i^{(n)} = \sum_{p=0}^{n} \sum_{k=0}^{k_{\max}} H_i^{(n,p,k)} x^p \rho^{-k} \,, \quad i = 1, 2, 3, 4 \,. \tag{4.53}$$

where $H_i^{(n,p,k)}$ are the constant coefficients to solve for when plugging the correction Eq. (4.48) into the perturbed EOM 4.42.

Finally, the asymptotic conditions become

$$H_1^{(n,0,0)} = 0 \,, \quad H_3^{(n,0,0)} = H_4^{(n,0,0)} = -\frac{H_3^{(n,0,1)}}{M} \,, \quad H_2^{(n,0,0)} = -\frac{H_3^{(n,0,0)}}{2} \,, \tag{4.54}$$

As mentioned in the introduction, this metric correction enables the study of black holes of any spin. The authors carried out a study about the convergence of the H_i functions (see appendix D in [6]) and found that for functions of order fourteen in χ, results for $\rho \geq \rho_+$ are accurate for spins up to 0.7.

As mentioned before, the metric perturbation of this thesis not only accounts for the six-derivative corrections to the action Eq. (2.6), but also its eight-derivative corrections. Therefore, the H_i functions of this thesis have two parts

$$H_i = H_i^{(6)} + H_i^{(8)}\,, \tag{4.55}$$

such that the correction to the metric becomes $\ell^4 g^{(6)}_{\mu\nu} dx^\mu dx^\nu + \ell^6 g^{(8)}_{\mu\nu} dx^\mu dx^\nu$ with the eight-derivative correction following the general scheme Eq. (4.48). In essence, solving the EOM of this thesis means inserting the expressions for $\ell^4 g^{(6)}_{\mu\nu} dx^\mu dx^\nu$ and $\ell^6 g^{(8)}_{\mu\nu} dx^\mu dx^\nu$ into the perturbed EOM Eqs. (4.42) and (4.43), via the trace-reverse metric perturbation, to find out the constant coefficients in $H_i^{(6)}$ and $H_i^{(8)}$, respectively. This was accomplished by first implementing Eqs. (4.42) to (4.44) and (4.48) with xCoba, and then using this implementation as input for the Mathematica notebook provided by Ref. [6]. The $H_i^{(6)}$ coefficients obtained as output agree with [6], and the $H_i^{(8)}$ coefficients obtained agree with the continuation work [12].

5 Properties of the corrected Kerr Black Hole

This section studies properties of the Kerr black hole, specifically the outer horizon[9] and ergosphere of a Kerr black hole corrected as described in section 4 . This study has been carried out following the steps of section four in Ref. [6], such that the results coming from the action's six-derivative corrections are reproduced, whereas the results from the eight-derivative corrections are original work.

5.1 Horizon

As mentioned in section 4.2, the coordinates used in this thesis lead to a horizon defined by $\Delta = 0$. Its solutions are the roots

$$\rho_\pm = M(1 \pm \sqrt{1-\chi^2}) \tag{5.56}$$

where ρ_- and ρ_+ correspond to the inner and outer horizon, respectively.
The choice of coordinates allows for this simple form for the horizon. In similar works previous to Ref. [6], other choices of coordinates resulted in complexity, which probably discouraged a thorough study of the event horizon.

[9] also called event horizon, or simply horizon

According to Hawking's rigidity theorem, the event horizon of a stationary, asymptotically flat black hole spacetime is a Killing horizon [25], that is, a null hypersurface whose Killing vector field (see discussion below Eq. (5.58)) vanishes [6]. Therefore, to study the (corrected) horizon, one must first ensure it obeys the rigidity theorem.

5.1.1 Killing horizon

First, it was proven that the hypersurface created by $\rho = \rho_+$ is null. In practice, this translates into showing that the determinant of the induced metric at some constant ρ, evaluated at $\rho = \rho_+$, is zero. Starting with the induced metric:

$$g_{\mu\nu}\,|_{\rho=\text{const}} = \\ = \begin{pmatrix} -\left(1-\frac{2M\rho}{\Sigma}-H_1\right) & 0 & -\left(1+H_2\right)\frac{2Ma\rho(1-x^2)}{\Sigma} \\ 0 & (1+H_3)\,\frac{\Sigma}{1-x^2} & 0 \\ -\left(1+H_2\right)\frac{2Ma\rho(1-x^2)}{\Sigma} & 0 & (1+H_4)\left(\rho^2+a^2+\frac{2M\rho a^2(1-x^2)}{\Sigma}\right)(1-x^2) \end{pmatrix} \tag{5.57}$$

its determinant was computed by expanding along the third row

$$\begin{aligned} &\det\left(g_{\mu\nu}\,\big|_{\rho=\rho_+}\right) = g_{xx}\left(g_{tt}g_{\phi\phi}-g_{t\phi}^2\right)\,\Big|_{\rho=\rho_+} = \\ &= (1+H_3)\,\frac{\Sigma}{1-x^2}\times\left[\frac{(-1+x^2)(-2(1+H_4)M\rho_+-(-1+H_1-H_4)(\rho_+^2+a^2x^2))}{(\rho_+^2+a^2x^2)^2}\right. \\ &\left.\times\,\frac{(\rho_+^4+a^4x^2+a^2\rho_+(2M+\rho_++(-2M+\rho_+)x^2))}{(\rho_+^2+a^2x^2)^2}-\frac{4a^2(1+2H_2)M^2\rho_+^2(-1+x^2)^2}{(\rho_+^2+a^2x^2)^2}\right] = \\ &= 0+\mathcal{O}(H_i^2)\,, \end{aligned} \tag{5.58}$$

and because the metric is corrected up to order ℓ^6, only the terms linear in the H_i functions are kept. The next step was to show that the Killing field at the horizon vanishes. A Killing vector field[10] on a manifold indicates the flow under which the metric remains constant. Consequently, the dimensions of a body following such flow would not get distorted. These concepts can be mathematically expressed using the Lie derivative $\mathcal{L}_B A$, as it computes the change of a tensor field A along the path indicated by another vector field B. Therefore, any Killing vector field K fulfills

$$\mathcal{L}_K\, g_{a\,b} = \nabla_b K_a + \nabla_a K_b = 0\,. \tag{5.59}$$

[10] sometimes called a Killing vector.

In principle, one would calculate the Killing vectors of a manifold using this equation. However, the metric used in this thesis converts this task into a laborious one. Sometimes, an easier way is to examine the metric. Since the metric in this thesis does not depend on t or ϕ, two Killing vectors on the manifold are the basis vectors ∂_t and ∂_ϕ, which Ref. [26] proves to be the only ones to consider here. Neither of these two fields vanish at the horizon, thus, a suitable linear combination of them must be found. From Refs. [25, 26], the most general Killing vector field at ρ_+ is then

$$\xi|_{\rho=\rho+} = (\partial_t + \Omega_H \partial_\phi)\,|_{\rho=\rho+}\,, \tag{5.60}$$

where the constant Ω_H represents the angular velocity at the horizon [27].
Ref. [6] states that the only angular velocity with which $\xi|_{\rho=\rho+}$ vanishes is

$$\Omega_H = \frac{a}{2M\rho_+}\left(1 + H_2 - H_4\right)\big|_{\rho=\rho_+}\,. \tag{5.61}$$

By combining expressions Eq. (5.60) and Eq. (5.61), the norm

$$\xi^2\big|_{\rho=\rho+} = \left(g_{tt} + 2g_{t\phi}\Omega_H + \Omega_H^2 g_{\phi\phi}\right)|_{\rho=\rho+} \tag{5.62}$$

was computed, first by including only the functions $H_i^{(6)}$, and then only the functions $H_i^{(8)}$. In both cases, the result was zero, as expected. Hence, the metric used in this thesis leads to a Killing horizon.

5.1.2 Angular velocity

The angular velocity can be conveniently expressed as a sum of three terms

$$\Omega_H = \frac{\chi}{2M\left(1+\sqrt{1-\chi^2}\right)} + \frac{\ell^4}{M^5}\lambda_{\rm ev}\,\Delta\Omega_H^{(6,{\rm ev})} + \frac{\ell^6}{M^7}\left(\epsilon_1\,\Delta\Omega_H^{(8,1)} + \epsilon_2\,\Delta\Omega_H^{(8,2)}\right)\,. \tag{5.63}$$

The first term is the angular velocity according to the Kerr solution, which was reproduced by expanding $a/2M\rho_+$ from Eq. (5.61). The second and third terms are the six and eight-derivative corrections to this Kerr part. They were reproduced and obtained by expanding $(a/2M\rho_+)(H_2^{(6)} - H_4^{(6)})$ and $(a/2M\rho_+)(H_2^{(8)} - H_4^{(8)})$ (also from Eq. (5.61)), respectively. The dimensionless coefficients $\Delta\Omega_H^{(i,j)}$ can be found in Eq. (D.1), Eq. (D.2) and Eq. (D.3). Note that these coefficients are multiplied by relevance factors $(\ell^{i-2}/M^k)\,c_j$, from which two observations can be made. i) The effect of the coefficients is larger for smaller masses and vice-versa. ii) Despite the coefficients difference in order, and unless ϵ_1 and ϵ_2 take exorbitant values, with these factors the six and eight-derivative angular velocity corrections are not of the same size, which agrees with the EFT philosophy.
In this thesis, all properties are expressed according to this three-term scheme, like in Ref. [6]. As mentioned in the introduction of this chapter, the first and second terms are always reproduced, while the third term is an original result.

It is of interest to examine the relation between the angular velocity and a parity transformation. Starting with Eq. (5.61), the H_i functions can be separated into their even and odd parts

$$\Omega_H = \frac{a}{2M\rho_+}\left(1 + H_2^{(\text{ev})} + H_2^{(\text{odd})} - H_4^{(\text{ev})} - H_4^{(\text{odd})}\right)\Big|_{\rho=\rho_+}\,, \tag{5.64}$$

where $H_2^{(\text{ev})} = H_2^{(6,\text{ev})} + H_2^{(8,1)} + H_2^{(8,2)}$ and $H_2^{(\text{odd})} = H_2^{(6,\text{odd})} + H_2^{(8,3)}$.
After the parity transformation, the even H_i functions remain invariant, while the odd ones change their sign. The horizon radius, Eq. (4.46), is not affected by the change of sign of χ, however, a changes sign. The transformation yields a turned, upside-down black hole with a rotation of the same angular speed but in the opposite direction. Therefore, the mentioned sign change implies that the odd functions cancel out. This conclusion agrees with the three-term expansion, where all the relevant powers of χ are odd and there are no "odd" coupling constants.

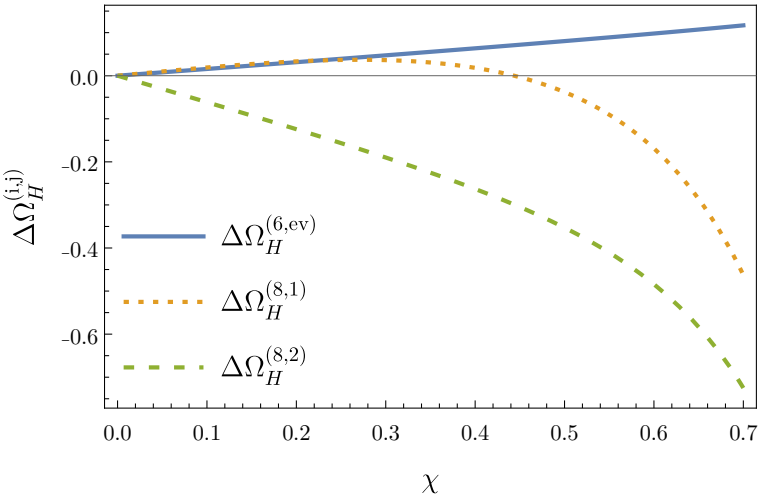

Figure 1: Corrections to the angular velocity associated with the six and eight-derivative corrections to the action.

Fig. 1 presents the coefficients $\Delta\Omega_H^{(i,j)}$. This plot was generated by including H_i functions up to order fifteen in χ, which in agreement with the convergence study mentioned in section 4.2, yield accurate results for $\chi = 0.7$. One observes that the effect of the coefficients $\Delta\Omega_H^{(6,\text{ev})}$ and $\Delta\Omega_H^{(8,2)}$ increases with χ. Moreover, $\Delta\Omega_H^{(8,2)}$ rapidly decreases beyond $\chi = 0.60$, while $\Delta\Omega_H^{(6,\text{ev})}$ remains approximately linear. The coefficient $\Delta\Omega_H^{(8,1)}$ coincides with the $\Delta\Omega_H^{(6,\text{ev})}$, at low values of χ, but around $\chi = 0.30$, it decreases non-linearly.

5.1.3 Surface gravity

The surface gravity κ of a Killing horizon is the force, applied from infinity, needed to keep a unit mass at rest on that horizon[11]. This is mathematically expressed as

$$\xi^a \nabla_a \xi^b|_{\rho=\rho_+} = \kappa \xi^b|_{\rho=\rho_+} \tag{5.65}$$

where $\xi|_{\rho=\rho_+}$ are the Killing vectors at the horizon Eq. (5.60) with Eq. (5.61). Here, the coordinates used in this thesis are singular at the horizon. Ref. [6] solves this issue by using a procedure proposed in [28], arriving at the following result

$$\begin{aligned}\kappa = \frac{(\rho_+ - M)}{2M\rho_+}\Bigg[1 + H_2 - \frac{H_3}{2} - \frac{H_4}{2} \\ + M^2\rho_+^2 \frac{\partial_\rho\left(-H_1\Sigma + a^2(1-x^2)(2H_2 - H_4)\right) + 2\left(\rho_+ - M\right)\left(H_4 - 2H_2\right)}{\left(\rho_+ - M\right)\left(\rho_+^2 + a^2x^2\right)^2}\Bigg]\Bigg|_{\rho=\rho_+}.\end{aligned} \tag{5.66}$$

In the three-term scheme, the surface gravity reads

$$\kappa = \frac{\sqrt{1-\chi^2}}{2M\left(1+\sqrt{1-\chi^2}\right)} + \frac{\ell^4}{M^5}\lambda_{\rm ev}\,\Delta\kappa^{(6,\rm ev)} + \frac{\ell^6}{M^7}\left(\epsilon_1\,\Delta\kappa^{(8,1)} + \epsilon_2\,\Delta\kappa^{(8,2)}\right). \tag{5.67}$$

where the first term corresponds to the expansion of $(\rho_+ - M)/2M\rho_+$ in Eq. (5.67), and the second and third terms to the expansion of the bracket. The coefficients $\Delta\kappa^{(i,j)}$ can be found in Eq. (D.4), Eq. (D.5) and Eq. (D.6). Three observations can be made. i) This result agrees with the zeroth law of Black Hole mechanics, which states that the horizon surface gravity of a stationary black hole spacetime is constant [26, 29]. ii) Due to the even powers of χ in the Kerr part and the coefficients, the surface gravity is invariant under parity transformations. iii) It is known that extremal black holes have zero surface gravity [11]. The Kerr part of the three-term expansion maintains this property, but not the coefficients. This suggests that in this thesis, extremality is reached at χ values beyond ± 1 [6]. However, this is not possible for the metric of this thesis, since the horizon would not exist, see Eq. (4.46); violating Penrose's weak cosmic censorship hypothesis, which asserts that naked singularities do not exist [30]. This observation does not necessarily mean that extremal black holes cannot be described by other metrics.

Fig. 2 presents the coefficients $\Delta\kappa^{(i,j)}$, which was generated with H_i functions up to order fifteen. One can observe that correction $\Delta\kappa^{(6,\rm ev)}$ follows a slow downward trend with a change of sign at $\chi = 0.5$. In contrast, $\Delta\kappa^{(6,\rm ev)}$, $\Delta\kappa^{(8,1)}$ and $\Delta\kappa^{(8,2)}$ never change their sign. Coefficient $\Delta\kappa^{(8,1)}$ stays approximately constant up to $\chi = 0.45$, from which it increases rapidly. Coefficient $\Delta\kappa^{(8,2)}$ begins at a null value and increases rapidly throughout the whole plot. It surpasses $\Delta\kappa^{(6,\rm ev)}$ and $\Delta\kappa^{(8,2)}$ at the χ values of 0.2 and 0.42, respectively.

[11] Ref. [26] gives an alternative and more mathematical definition.

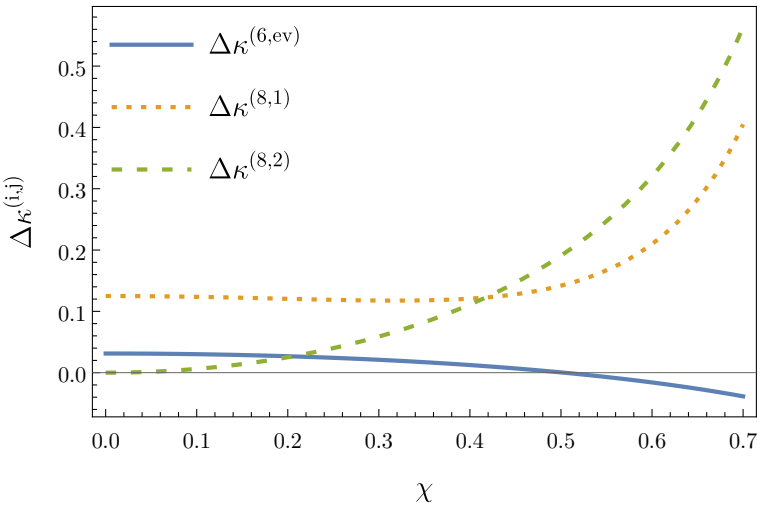

Figure 2: Corrections to the surface gravity associated with the six and eight-derivative corrections to the action.

Surface gravity is an important concept. It appears in the Hawking radiation temperature at the horizon of a Kerr black hole [6]

$$T_H = \frac{\kappa}{2\pi}\,, \tag{5.68}$$

which relates a geometrical property of spacetime (surface gravity) with a thermal property of quantum fields (temperature). From this equation, one can deduce that extremal black holes do not radiate, which is a well-known result.

5.1.4 Geometry

For the study of the area and shape of the horizon, one has to use the induced metric at the horizon:

$$ds_H^2 = (1+H_3)\,|_{\rho=\rho_+}\frac{\rho_+^2+a^2x^2}{1-x^2}dx^2 + (1+H_4)\,|_{\rho=\rho_+}\frac{4M^2\rho_+^2\,(1-x^2)}{\rho_+^2+a^2x^2}d\phi^2\ . \tag{5.69}$$

5.1.4.1 Area

The area of the horizon is given by

$$A_H = 4\pi M\rho_+\int_{-1}^{1}dx\left(1+\frac{H_3}{2}+\frac{H_4}{2}\right)\Big|_{\rho=\rho_+}\,, \tag{5.70}$$

in the three-term notation, it reads

$$A_H = 8\pi M^2\left(1+\sqrt{1-\chi^2}\right)+\frac{\pi\ell^4}{M^2}\lambda_{\mathrm{ev}}\,\Delta A^{(6,\mathrm{ev})}+\frac{\pi\ell^6}{M^4}\left(\epsilon_1\,\Delta A^{(8,1)}+\epsilon_2\,\Delta A^{(8,2)}\right), \tag{5.71}$$

where the Kerr part, comes from the expansion of $4\pi M\rho_+ 2$, and the second and third terms come from the expansion of $4\pi M\rho_+ \int_{-1}^{1} dx \left(\frac{H_3}{2} + \frac{H_4}{2}\right)\Big|_{\rho=\rho_+}$. The coefficients $\Delta A^{(i,j)}$ can be found in Eqs. (D.7) to (D.9). Once again, the even powers of χ on the whole solution make the area invariant under parity transformations.

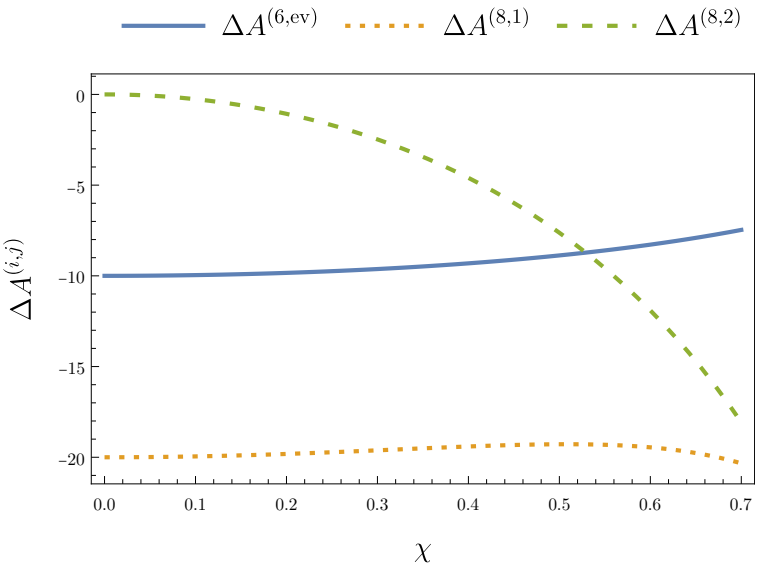

Figure 3: Corrections to the area of the horizon associated with the six and eight-derivative corrections to the action.

Fig. 3 shows the profile of the coefficients $\Delta A^{(i,j)}$, which was generated with H_i functions up to order fifteen. One can see that the behavior of the three curves is very different. The coefficients $\Delta A^{(6,\mathrm{ev})}$ diminish in a non-linear way. Coefficients $\Delta A^{(8,1)}$ remain approximately constant, with a small peak between $\chi = 0.3$ and $\chi = 0.7$. The coefficients $\Delta A^{(8,2)}$ start at a null value and increase throughout the plot, intersecting $\Delta A^{(6,\mathrm{ev})}$ at $\chi = 0.52$, these influence the size of the horizon. Depending on the sign of the relevant factors, they translate into increases and decreases in the area and vice-versa.

5.1.4.2 Shape

A good way to visualize the shape of the event horizon is by embedding it on a 3D Euclidean space. In terms of Cartesian coordinates, the isometric embedding of any axisymmetric surface is done as follows:
The x and z Cartesian coordinates are given by

$$x = f(x') \sin\frac{\pi}{2}\,, \quad z = g(x')\,, \tag{5.72}$$

where x' represents the x Boyer-Linqvist coordinate, introduced to avoid confusion with the x Cartesian coordinate. The functions $f(x')$ and $g(x')$ are determined by imposing the

metric

$$ds^2 = \left[(f')^2 + (g')^2\right] dx'^2 + f^2\, d\phi^2 \,. \tag{5.73}$$

When considering the metric, Eq. (5.69), $f(x')$ and $g(x')$ are given by

$$f(x') = 2M\rho_+ \left(1 + \frac{H_4}{2}\right)\Big|_{\rho=\rho_+} \left(\frac{1 - x'^2}{\rho_+^2 + a^2 x'^2}\right)^{1/2} , \tag{5.74}$$

$$g(x') = \int dx' \left[(1 + H_3)\,|_{\rho=\rho_+} \frac{\rho_+^2 + a^2 x'^2}{1 - x'^2} - (f')^2\right]^{1/2} , \tag{5.75}$$

where the square root of $1 + H_4$ was approximated with a Taylor expansion. Note that this embedding is valid for $g_{xx} \geq (f')^2$, which is not fulfilled for some values of x' and χ, as verified in the figures below.
For the reproduction and generation of horizon shapes, Eqs. (5.72), (5.74) and (5.75) were implemented. The reproductions of the six-derivative shapes do not completely agree with the results of Ref. [6], in which all parameters except for the order of the H_i functions are specified. No bugs were found in the implementation; however, it was seen that the results get more similar to the ones in Ref. [6] as the order of the functions increases and χ decreases.

Fig. 4 presents the Kerr horizon and its deformations due to the even parts of the $H_i^{(6)}$ functions. The Kerr solution is presented as a black dashed curve. Results including the corrections are presented as full lines, where darker purple colours correspond to larger values of the coupling, $\frac{\ell^4}{M^4}\lambda_{\text{ev}} = -0.4, -0.2, 0.2, 0.4$. The left subfigure was generated with $\chi = 0.65$, as in [6], and an H_i order of fifteen, as used in [6] for previous results. Its curves intersect around $z = \pm 1.4$. However, the counterpart result in the reference consists of concentric curves. The right subfigure, which was generated with $\chi = 0.18$ and an H_i order of twenty-five, reproduces this concentricity much better. Moreover, its colour gradient is in the right order, with bigger coupling values leading to smaller radiuses and vice-versa. Notice that both subfigures are incomplete around the poles. Those missing points correspond to cases where the square root of $g(x')$ is negative, as mentioned below Eq. (5.75).

Fig. 5 presents Kerr horizon's deformations caused by the odd parts of the $H_i^{(6)}$ functions. With the coupling $\frac{\ell^4}{M^4}\lambda_{\text{odd}} = 0.6$, and the colour gradient from light to darker green corresponds to the mass values $M = 0.75, 0.9, 1.1, 1.4$. The left subfigure was generated with $\chi = 0.65$, as in [6], and an H_i order of fifteen, as in [6] for previous results. Althought this subfigure does not look exactly like its couterpart in Ref. [6], they both follow the same trend. For higher masses, the shape is oblate, very similar to the exact horizon. However, as the mass decreases, the horizon gets smaller, its upper part gets flatter, but its lower part gets rounder. Regarding the colour gradient, and as opposed to the even six-derivative deformations, smaller coupling values lead to smaller horizons. In order to

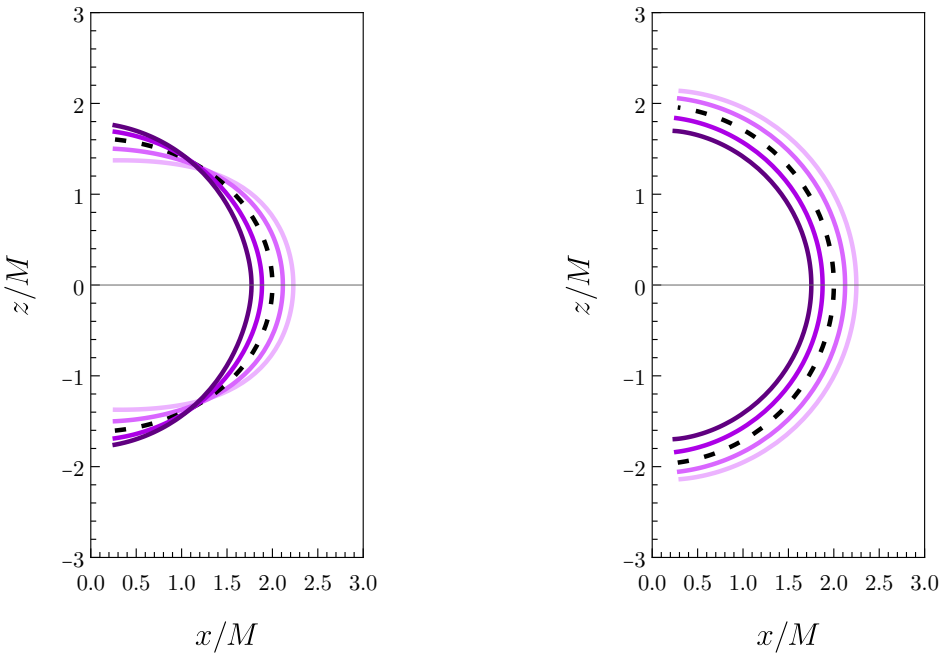

Figure 4: Isometric embedding of the Kerr horizon and its deformations due to the even part of the six-derivative corrections. The mass was set to one, the black dashed curve is the Kerr horizon, and from light to darker purple, the value of the couplings is $\frac{\ell^4}{M^4}\lambda_{\rm ev} = -0.4, -0.2, 0.2, 0.4$. The left subfigure was generated with $\chi = 0.65$ and an H_i order of fifteen, and the right subfigure was generated with $\chi = 0.18$ and an H_i order of twenty-five.

present more complete curves, χ was lowered to 0.25 and the H_i order was increased to 25, presented in the left subfigure, where the same trend applies.

Fig. 6 presents the Kerr horizon and its deformations due to the eight-derivative corrections. The left and middle subfigures focus on the deformations related to ϵ_1 and ϵ_2, respectively. They were generated with $\chi = 0.18$, an H_i order of twenty-five, and couplings $\frac{\ell^6}{M^6}\epsilon_1 = -0.4, -0.2, 0.2, 0.4$ and $\frac{\ell^6}{M^6}\epsilon_2 = -4, -2, 2, 4$. One can observe that while the left subfigure follows the same trend as the even six-derivative deformations, the right subfigure in 4, the middle panel shows a lateral flattening for bigger coupling values and a lateral elongation for smaller coupling values. Both follow the same colour gradient as in the six-derivative deformations. The right subfigure describes the deformations related to ϵ_3. It was generated with $\chi = 0.30$, an H_i order of twenty-five, $\frac{\ell^6}{M^6}\epsilon_3 = 0.6$, and masses $M = 0.75, 0.9, 1.1, 1.4$. Like in the odd six-derivative deformations, the shape is oblate for higher masses. However, as the mass decreases, the horizon gets smaller with a flatter upper part, and the sides flatten and tilt towards the origin.

It is of interest to discuss the relation between the symmetry of the shapes and parity transformations. These leave the shapes coming from even corrections invariant, which the ovals associated to $\lambda_{\rm ev}$, ϵ_1 and ϵ_2 (Fig. 4 and left and middle subfigures in Fig. 6),

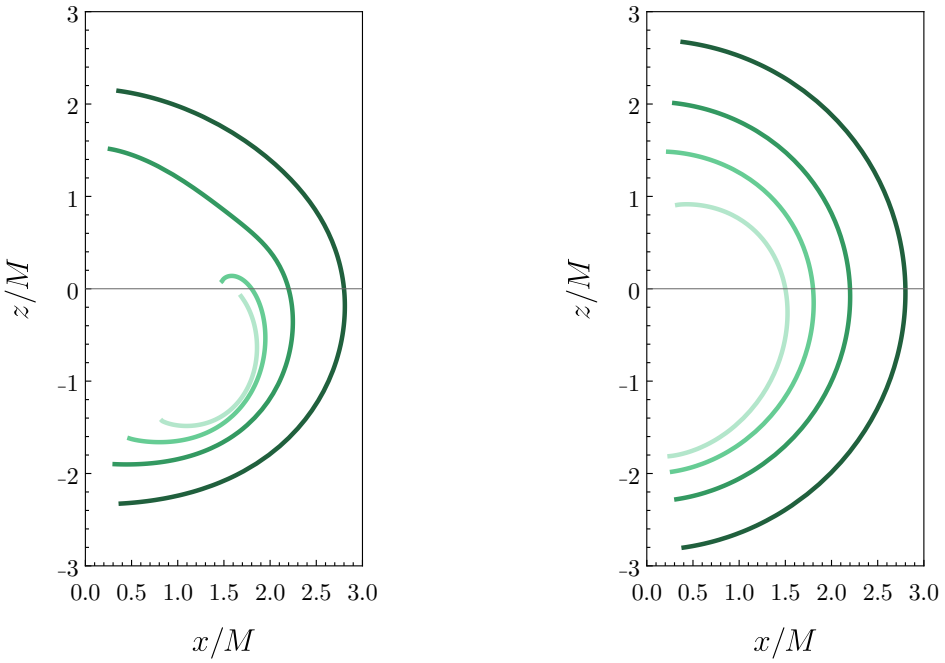

Figure 5: Isometric embedding of Kerr horizon's deformations due to the odd part of the six-derivative corrections. The coupling $\frac{\ell^4}{M^4}\lambda_{\rm odd}$ was set to 0.6, and from light to darker green, the value of the mass is $M = 0.75, 0.9, 1.1, 1.4$. The left subfigure was generated with $\chi = 0.65$ and an H_i order of fifteen, and the right subfigure was generated with $\chi = 0.18$ and an H_i order of twenty-five.

agree with. In contrast, the shapes coming from odd corrections transform in such a way that it is evident that they are upside down and rotated. Given that the induced metric Eq. (5.69) does not depend on ϕ, the only possibility left is an asymmetry between the upper and lower parts of the shapes, which is the case of the ones associated with $\lambda_{\rm odd}$ and ϵ_3 in Fig. 5 and the right subfigure in Fig. 6, respectively.

5.2 Ergosphere

The ergosphere radius of any axisymetric metric is defined by the condition $g_{tt} = 0$. For the Kerr metric, this condition yields

$$1 - \frac{2M\rho_{\rm erg}^{\rm (Kerr)}}{\Sigma} = 0\,, \tag{5.76}$$

therefore, the Kerr ergosphere radius is given by

$$\rho_{\rm erg}^{\rm (Kerr)} = M\left(1 + \sqrt{1 - \chi^2 x^2}\right)\,. \tag{5.77}$$

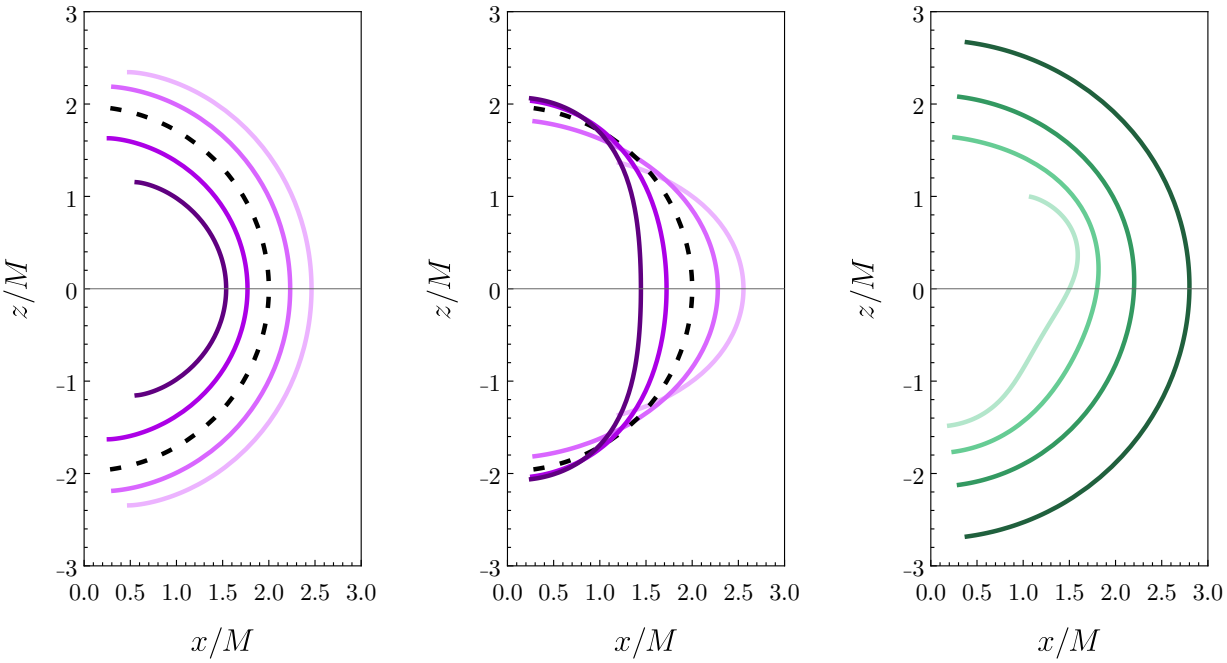

Figure 6: Isometric embedding of the Kerr horizon and its deformations due to the eight-derivative corrections up to order twenty-five. The left and middle subfigures show the deformations related to ϵ_1 and ϵ_2, respectively. For both of them, the mass was set to one, $\chi = 0.18$, and the black dashed curve is the Kerr horizon. From light to darker purple, the value of the couplings is $\frac{\ell^6}{M^6}\lambda_{\rm ev} = -0.4, -0.2, 0.2, 0.4$ and $\frac{\ell^6}{M^6}\lambda_{\rm ev} = -4, -2, 2, 4$, respectively. The right subfigure shows the deformations related to ϵ_3. It was generated with $\chi = 30$, an H_i order of twenty-five, $\frac{\ell^6}{M^6}\epsilon_3 = 0.6$, and masses $M = 0.75, 0.9, 1.1, 1.4$.

However, for the metric used in this thesis, $g_{tt} = 0$ reads

$$1 - \frac{2M\rho_{\rm erg}}{\Sigma} = H_1\,, \tag{5.78}$$

with which the three-term expansion of $\rho_{\rm erg}$ was derived as follows:

The correction to $\rho_{\rm erg}$ is perturbative, and H_1 is small. Therefore, as a first step, it is valid to perform a first-order Taylor expansion of the left-hand side about $\rho_0 = \rho_{\rm erg}^{\rm (Kerr)}$ and evaluate H_1 at $\rho_{\rm erg}^{\rm (Kerr)}$:

$$1 + \frac{2M\left(\rho_{\rm erg} - \rho_{\rm erg}^{\rm (Kerr)}\right)\left[\left(\rho_{\rm erg}^{\rm (Kerr)}\right)^2 - M^2x^2\chi^2\right]}{\left[\left(\rho_{\rm erg}^{\rm (Kerr)}\right)^2 + M^2x^2\chi^2\right]^2} - \frac{2M\rho_{\rm erg}^{\rm (Kerr)}}{\left(\rho_{\rm erg}^{\rm (Kerr)}\right)^2 + M^2x^2\chi^2} = H_1(x, \rho_{erg})\,. \tag{5.79}$$

In this way, $\rho_{\rm erg}$ can be isolated:

$$\rho_{\rm erg} = \rho_{\rm erg}^{\rm (Kerr)} + \frac{\left[\left(\rho_{\rm erg}^{\rm (Kerr)}\right)^2 + M^2x^2\chi^2\right]^2}{2M\left[\left(\rho_{\rm erg}^{\rm (Kerr)}\right)^2 - M^2x^2\chi^2\right]}\left(H_1(x,\rho_{erg}) + \frac{2M\rho_{\rm erg}^{\rm (Kerr)}}{\left(\rho_{\rm erg}^{\rm (Kerr)}\right)^2 + M^2x^2\chi^2} - 1\right) \tag{5.80}$$

where the second term is the correction. By plugging Eq. (5.77) into this sum, the following three-term expansion was obtained

$$\begin{aligned}\rho_{\rm erg} =& M\left(1+\sqrt{1-\chi^2x^2}\right) \\ &+ \frac{\ell^4}{M^3}\left(\lambda_{\rm ev}\Delta\rho^{(6,{\rm ev})} + \lambda_{\rm odd}\Delta\rho^{(6,{\rm odd})}\right) + \frac{\ell^6}{M^5}\left(\epsilon_1\Delta\rho^{(8,1)} + \epsilon_2\Delta\rho^{(6,2)}\right)\end{aligned} \tag{5.81}$$

The coefficients $\Delta\rho^{(6,j)}$ can be found in Eq. (D.10) and Eq. (D.11). They come from considering $H_1^{(6)}(x,\rho_{\rm erg})$, and agree with [6]. Coefficients $\Delta\rho^{(8,j)}$ can be found in Eq. (D.12) and Eq. (D.12); and they come from considering $H_1^{(8)}(x,\rho_{\rm erg})$.

It is known that the ergosphere of the Kerr metric overlaps the outer horizon at its north and south poles. It was found that the metric used in this thesis maintains this property. With the poles given by $x = \pm 1$, $\rho_{\rm erg}$ (Eq. (5.77)) becomes ρ_+ (Eq. (5.56)), and the coefficients $\Delta\rho^{(i,j)}$ vanish.

To study the shape of the ergosphere, one uses the induced metric for $\rho = \rho_{\rm erg}$ at constant time:

$$\begin{aligned}ds^2_{\rm erg} =& (1+H_3)\,\Sigma\left(\frac{1}{\Delta}\left(\frac{d\rho_{\rm erg}}{dx}\right)^2 + \frac{1}{1-x^2}\right)dx^2 \\ &+ (1+H_4)\left(\rho^2 + a^2 + \frac{2M\rho a^2(1-x^2)}{\Sigma}\right)(1-x^2)d\phi^2\Big|_{\rho=\rho_{\rm ert}(x)},\end{aligned} \tag{5.82}$$

Like in the study of the horizon shape, 5.1.4.2, the visualization technique used is the isometric embedding on a 3D Euclidean space. By following the steps in 5.1.4.2, the $f(x')$ and $g(x')$ functions were found to be

$$f(x') = \left(1+\frac{H_4}{2}\right)\left[\left(\rho^2 + a^2 + \frac{2M\rho a^2(1-x'^2)}{\Sigma}\right)(1-x'^2)\right]^{1/2}\Big|_{\rho=\rho_{\rm ert}(x\prime)} \tag{5.83}$$

$$g(x') = \int dx'\left[(1+H_3)\,\Sigma\left(\frac{1}{\Delta}\left(\frac{d\rho_{\rm erg}}{dx\prime}\right)^2 + \frac{1}{1-x'^2}\right)dx'^2 - (f')^2\right]^{1/2}\Big|_{\rho=\rho_{\rm ert}(x')}, \tag{5.84}$$

were again this embedding fails for the values of x and χ that lead to a negative square root in $g(x')$.

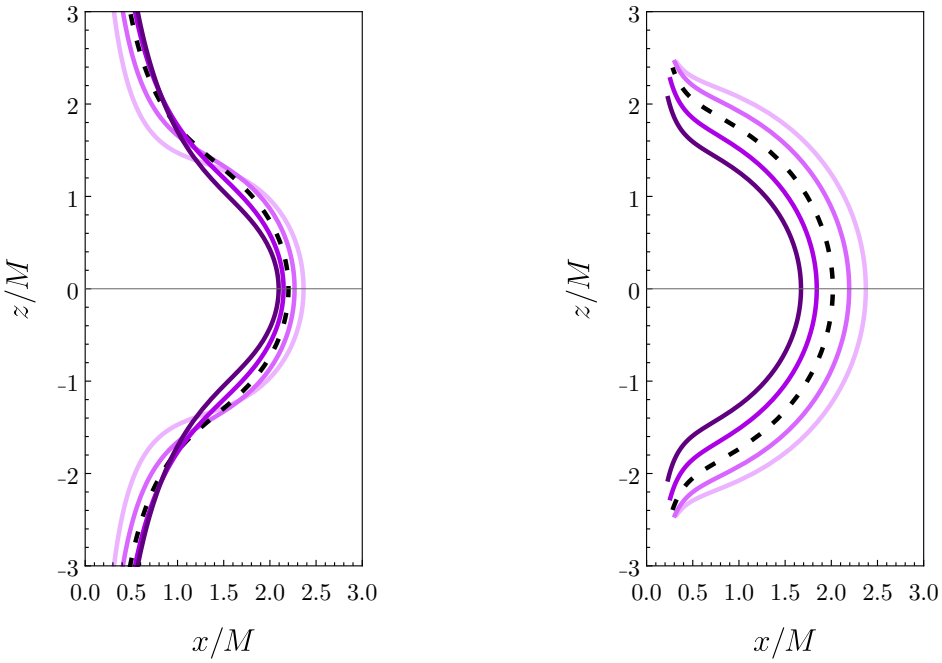

Figure 7: Isometric embedding of the Kerr ergosphere and its deformations due to the even part of the six-derivative corrections. The mass was set to one, the black dashed curve is the Kerr horizon, and from light to darker purple, the value of the couplings is $\frac{\ell^4}{M^4}\lambda_{\rm ev} = -0.6, -0.3, 0.3, 0.6$. The left subfigure was generated with $\chi = 0.65$ and an H_i order of fifteen, and the right subfigure was generated with $\chi = 0.18$ and an H_i order of twenty-five.

Fig. 7 presents the Kerr ergosphere and its deformations due to the even parts of the $H_i^{(6)}$ functions. The plot style is the same as in the even horizon deformation from subsection 5.1.4.2, with the Kerr solution presented as a black dashed, corrections presented as full lines, and darker purple colours corresponding to larger values of the coupling, $\frac{\ell^4}{M^4}\lambda_{\rm ev} = -0.6, -0.3, 0.3, 0.6$. The left subfigure was generated with $\chi = 0.65$, as in [6], and an H_i order of fifteen, again as used in [6] for previous results. The curves of this subfigure follow the same trend as their counterparts in the reference, as they all intersect on the upper and lower parts and the colour gradient is in agreement. Still, those intersections are supposed to happen a bit beyon $z = \pm 2$, and the curves are supposed to intersect this z axis at $z = \pm 2.5$, approximately. The right subfigure was generated with $\chi = 0.18$ and an H_i order of twenty-five, and although it seems to reproduce better the intersections of the reference counterpart, it is still an inconclusive result because of the imaginary coordinates around the poles. When confronting these left and right subfigures one can notice that as the spin increases, the closer to the Kerr ergosphere the curves get.

Fig. 8 presents Kerr ergosphere's deformations caused by the odd parts of the $H_i^{(6)}$ functions. With the coupling $\frac{\ell^6}{M^6}\lambda_{\rm odd} = 0.6$, and the colour gradient from light to darker green corresponds to the mass values $M = 0.75, 0.9, 1.1, 1.4$. The left subfigure was generated

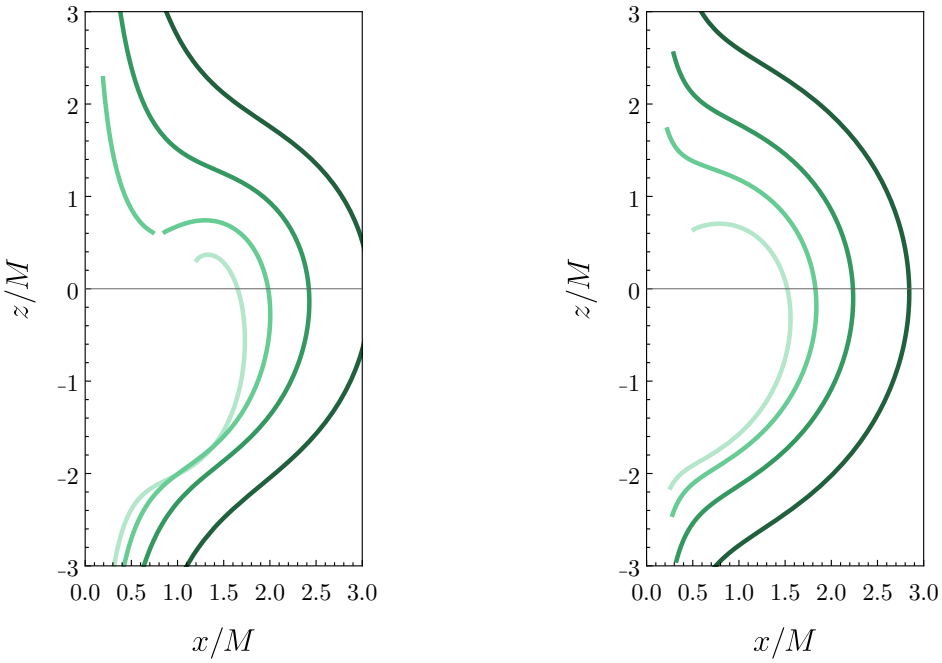

Figure 8: Isometric embedding of Kerr ergosphere's deformations due to the odd part of the six-derivative corrections. The coupling $\frac{\ell^4}{M^4}\lambda_{\text{odd}}$ was set to 0.6, and from light to darker green, the value of the mass is $M = 0.75, 0.9, 1.1, 1.4$. The left subfigure was generated with $\chi = 0.65$ and an H_i order of fifteen, and the right subfigure was generated with $\chi = 0.25$ and an H_i order of twenty-five.

with $\chi = 0.65$, as in [6], and an H_i order of fifteen, again as in [6] for previous results. Although this subfigure does not look exactly like its couterpart in the reference, they both follow the same trend. The colour gradient is in agreement, none of the curves intersect, but all of them take the shape of a spinning top, with the smaller masses having flatter upper parts. As in the previous figure, some of the curves intersect the z axis at values higher than in the counterpart, and some others are even incomplete around the poles. To fix these issues, χ was lowered to 0.25 and the H_i order was increased to 25, presented in the left subfigure. It has the same colour gradient and lack of intersection as the previous left subfigure. Moreover, the two lightest curves seem to behave smoother. However, the mentioned issues are still present.

Fig. 9 presents Kerr's ergosphere and its deformations due to the eight-derivative corrections. The left and middle subfigures focus on the deformations related to ϵ_1 and ϵ_2, respectively. They were generated with $\chi = 0.18$, an H_i order of twenty-five, and couplings $\frac{\ell^6}{M^6}\epsilon_1 = -0.6, -0.3, 0.3, 0.6$ and $\frac{\ell^6}{M^6}\epsilon_2 = -2, -1, 1, 2$. The left subfigure is similar to its six-derivative counterpart in Fig.7, in shape, color gradient, and both being approximately concentric. Its curves seem to approach some asymptotic value beyond ± 3. In contrast, the curves of the middle figure get close to each other around $z = \pm 2$. While the curves with smaller couplings resemble the corresponding curves in the left panel, those with large

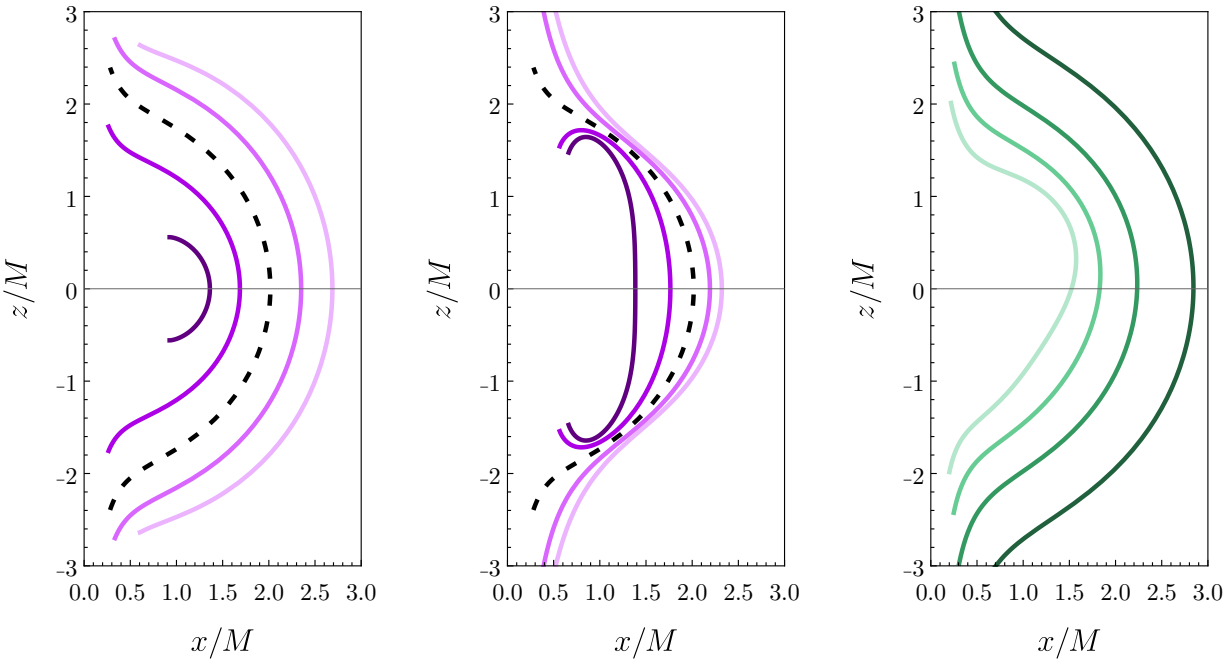

Figure 9: Isometric embedding of the Kerr ergosphere and its deformations due to the eight-derivative corrections up to order twenty-five. The left and middle subfigures show the deformations related to ϵ_1 and ϵ_2, respectively. For both of them, the mass was set to one, $\chi = 0.18$, and the black dashed curve is the Kerr horizon. From light to darker purple, the value of the couplings is $\frac{\ell^6}{M^6}\epsilon_1 = -0.6, -0.3, 0.3, 0.6$ and $\frac{\ell^6}{M^6}\epsilon_2 = -2, -1, 1, 2$. The right subfigure shows the deformations related to ϵ_3. It was generated with $\chi = 0.25$, an H_i order of twenty-five, $\frac{\ell^6}{M^6}\epsilon_3 = 0.6$, and masses $M = 0.75, 0.9, 1.1, 1.4$.

couplings bend back towards the origin, possibly because of convergence issues. The right subfigure describes the deformations related to ϵ_3. It was generated with $\chi = 30$, an H_i order of twenty-five, $\frac{\ell^6}{M^6}\epsilon_3 = 0.6$, and masses $M = 0.75, 0.9, 1.1, 1.4$. Like in the odd six-derivative deformations, Fig. 8, the shape is more similar to Kerr's ergosphere for higher masses. However, as the mass decreases, the shapes get smaller with a flatter upper part, and the lower parts flatten and tilt towards the origin.

All the curves in this subsection have a strange behaviour around the poles. This is in fact incompatible with the ergosphere meeting the horizon at the poles, as checked below Eq. (5.81). Some of these curves intersect the z axis at higher values compared to their counterparts in Ref. [6]. The rest of the curves are incomplete, with a few in this subgroup bending back towards the origin. As shown throughout this subsection, all these anomalies mitigate after increasing the order of the H_i functions and decreasing the value of χ, proving the necessity of using an exceptionally high χ order for the embedding considered (Eqs. (5.83) and (5.84)).

The conclusions about the relation between the symmetry of the shapes and parity trans-

formations drawn in section 5.1.4.2 apply here as well. The curves coming from even corrections (Fig. 7 and left and middle subfigures in Fig. 9) are symmetric and therefore parity-even. In contrast, the x dependance of the induced metric Eq. (5.82) leads to asymmetries, and therefore odd parity, in curves coming from odd corrections (Fig. 8 and right subfigure in Fig. 9).

Finally, by comparing the horizon deformations with the ergosphere ones, one can observe that while the former take oblate-like shapes, the latter look like spinning tops with a small elongation around both poles. This is indeed the behaviour of the of the Kerr horizon and ergosphere, meaning that the corrections do not lead to drastic changes, in turn meaning that the EFT philosofy is again present.

6 Conclusions

In chapter 2, the action of this thesis was constructed. The Einstein-Hilbert action was corrected with higher-derivative gravity in an effective field theory fashion. After discarding the curvature invariants that do not contribute to the equations of motion, the remaining corrections are even-parity and odd-parity operators containing six and eight derivatives. The Euler Lagrange equations suitable for these operators were derived in section 3.1. In section 5 and appendix A, these equations, along with convenient properties that derive from Ricci-flat spaces, were applied to the action, and the equations of motion were obtained. These equations of motion were solved by first performing a first-order perturbation on the Einstein tensor, in section 4.1, then deriving an ansatz for the six and eigh-derivative metric corrections for a rotating black hole, in section 4.1, and finally solving the resulting system of equation with the MATHEMATICA script provided by Ref.[6]. With this corrected metric, the properties of the horizon and ergosphere of a rotating black hole were studied.

There are several factors indicating that the eight-derivative results concerning the nature of the horizon, as well as the angular velocity, surface gravity, and area in that zone, are correct: i) They were obtained with the same codes that generate the exact and six-derivative results, which agree with Ref. [6]. ii) Along with the exact and six-derivative results, they agree with the following theoretical predictions: The horizon obeys Hawking's rigidity theorem and the zeroth law of black hole mechanics. It also rotates in the opposite direction after applying a parity transformation while its surface gravity and area remain invariant. The three-term expansions, which derive from well-known formulas, follow the effective field theory approach, as the Kerr term contributes the most and the eight-derivate term contributes the least due to the relevance factors. iii) All results were generated both with H_i functions of order fifteen and twenty-five. No differences were detected, implying that they converge at least in the χ range considered.

In contrast, convergence differences were observed in the shapes of the horizon and ergosphere. The six-derivative shapes follow the general trend of their counterparts in Ref. [6], especially trends regarding color gradients, and symmetries/asymmetries between the up-

per and lower parts. However, they are not in quantitative agreement despite thoroughly revising the implementation. One possible reason could be that an exceptionally high H_i order was required, but this could not be met because the generation of each subfigure required up to two days of computational time.

Despite the disagreement of the ergosphere shapes, the corresponding three-term expansion agrees with the well-known overlap with the event horizon at the poles. For any value of χ, the exact term takes the form of the event horizon radius, and the six and eight-derivative coefficients vanish.

The eight-derivative results behave quite differently from their six-derivative counterparts, especially concerning the horizon and ergosphere shapes. Even though the former's results are more heavily suppressed, this difference might lead to minor changes when comparing observables that include and exclude these new corrections.

A possible extension of this thesis would be the computation of Love numbers, which describe the linear deformation of a body experiencing tidal perturbations. Most of the literature studies Love numbers of General Relativity black holes, but with the advent of higher-derivative gravity, such works have to be adapted. Ref. [31] goes through the Love numbers computation for the case of a Kerr black hole. In this reference, as in similar works, the curvature tensors are written in terms of a special set of basis vectors known as the null tetrad. In this formalism, the metric is not perturbed, but the vectors of the null tetrad, the derivative operators, and the curvature tensors related to the tidal deformations. The result is a separable set of linear Partial Differential Equations called the Teutolski equations, whose solutions are the tidal deformations from which Love numbers come. A first step would consist of performing the mentioned perturbations taking into account the metric corrections in this thesis. Works [32, 33] derive the Teutolski equations valid for a Kerr background corrected with six-derivative curvature invariants. These works would have to be extended to include the eight-derivative corrections in those perturbations.

A Reproduction of the EOM associated to the eight-derivative correction $\mathcal{C}\tilde{\mathcal{C}}$

This section reproduces the terms

$$4\tilde{R}^{yazb}(\nabla_a\nabla_b\mathcal{C}) + 4R^{yazb}(\nabla_a\nabla_b\tilde{\mathcal{C}}) + \frac{1}{2}g^{yz}\tilde{\mathcal{C}}\mathcal{C} \tag{A.1}$$

from Ref. [10]. This sum is the EOM of $\mathcal{C}\tilde{\mathcal{C}}$, which, in turn, is one of the three eight-derivative corrections to the EH action of this thesis, as Eq. (2.6) shows. The derivation starts with an expansion that results from first applying the EL equations, Eq. (3.20), to $\mathcal{C}\tilde{\mathcal{C}}$, then setting the Ricci tensors and scalars to zero, and finally applying property iii) from section 5:

$$\begin{aligned}
&- \epsilon_{ghij}g^{yz}R_{abcd}R^{abcd}R_{ef}{}^{ij}R^{efgh} + 2\,\epsilon^{z}{}_{ade}R_{bc}{}^{de}R_{fghi}R^{fghi}R^{yabc} \\
&+ 2\,\epsilon_{fghi}R_{de}{}^{hi}R^{defg}R^{yabc}R^{z}{}_{abc} + 2\,\epsilon^{y}{}_{ade}R_{bc}{}^{de}R_{fghi}R^{fghi}R^{zabc} \\
&+ 4\,\epsilon_{efgh}R^{cdef}R^{yazb}(\nabla_a\nabla_bR_{cd}{}^{gh}) + 4\,\epsilon^{z}{}_{bch}R^{defg}R^{yabc}(\nabla_a\nabla^hR_{defg}) \\
&+ 4\,\epsilon^{y}{}_{bch}R^{defg}R^{zabc}(\nabla_a\nabla^hR_{defg}) + 8\,\epsilon_{efgh}R^{yazb}(\nabla_aR^{cdef})(\nabla_bR_{cd}{}^{gh}) \\
&+ 4\,\epsilon_{efgh}R^{cdef}R^{yazb}(\nabla_b\nabla_aR_{cd}{}^{gh}) + 2\,\epsilon^{z}{}_{fgh}R_{abcd}R^{abcd}(\nabla_e\nabla^hR^{yefg}) \\
&+ 2\,\epsilon^{y}{}_{fgh}R_{abcd}R^{abcd}(\nabla_e\nabla^hR^{zefg}) + 4\,\epsilon^{z}{}_{bch}R^{yabc}(\nabla_aR^{defg})(\nabla^hR_{defg}) \\
&+ 4\,\epsilon^{y}{}_{bch}R^{zabc}(\nabla_aR^{defg})(\nabla^hR_{defg}) + 4\,\epsilon^{z}{}_{fgh}R^{abcd}(\nabla_eR_{abcd})(\nabla^hR^{yefg}) \\
&+ 4\,\epsilon^{y}{}_{fgh}R^{abcd}(\nabla_eR_{abcd})(\nabla^hR^{zefg})\,.
\end{aligned} \tag{A.2}$$

The rest of the derivation consists of using the symmetries of the Levi-Civita and Riemann tensors, along with properties i) to iii) from section 5, to reduce this expansion to Eq. (A.1).

By the symmetries of the Levi-Civita and Riemann tensors, and property ii), the indices z and y in the $4\,\epsilon^{z}{}_{bch}R^{yabc}(\nabla_aR^{defg}\nabla^hR_{defg})$ and $4\,\epsilon^{z}{}_{bch}R^{defg}R^{yabc}(\nabla_a\nabla^hR_{defg})$ terms can be exchanged. Thus,

$$\begin{aligned}
&4\,\epsilon^{y}{}_{bch}R^{zabc}(\nabla_aR^{defg})(\nabla^hR_{defg}) + 4\,\epsilon^{z}{}_{bch}R^{yabc}(\nabla_aR^{defg})(\nabla^hR_{defg}) = \\
&= 8\,\epsilon^{y}{}_{bch}R^{zabc}(\nabla_aR^{defg})(\nabla^hR_{defg})\,,
\end{aligned} \tag{A.3}$$

$$\begin{aligned}
&4\,\epsilon^{z}{}_{bch}R^{defg}R^{yabc}(\nabla_a\nabla^hR_{defg}) + 4\,\epsilon^{y}{}_{bch}R^{defg}R^{zabc}(\nabla_a\nabla^hR_{defg}) = \\
&= 8\,\epsilon^{y}{}_{bch}R^{defg}R^{zabc}(\nabla_a\nabla^hR_{defg})\,,
\end{aligned} \tag{A.4}$$

where the covariant derivatives of the result $8\,\epsilon^{y}{}_{bch}R^{defg}R^{zabc}(\nabla_a\nabla^hR_{defg})$ can be exchanged. One can prove this commutation by first expanding the covariant derivative part of the result

$$\nabla_a\nabla^hR_{defg} = R_a{}^h{}_e{}^bR_{dbfg} + R_a{}^h{}_g{}^bR_{defb} - R_a{}^h{}_f{}^bR_{degb} - R_a{}^h{}_d{}^bR_{ebfg} + \nabla^h\nabla_aR_{defg}\,, \tag{A.5}$$

then writing the first four terms in this resulting expansion in terms of their Christoffel Symbols

$$\begin{aligned} &R_a{}^h{}_e{}^b R_{dbfg} = g_{gj} g^{hc} (\Gamma^b{}_{ci} \Gamma^i{}_{ae} - \Gamma^b{}_{ai} \Gamma^i{}_{ce} - \partial_a \Gamma^b{}_{ce} + \partial_c \Gamma^b{}_{ae}) \\ &(-\Gamma^j{}_{dk} \Gamma^k{}_{bf} + \Gamma^j{}_{bk} \Gamma^k{}_{df} + \partial_b \Gamma^j{}_{df} - \partial_d \Gamma^j{}_{bf}) \end{aligned} \tag{A.6}$$

$$\begin{aligned} &R_a{}^h{}_g{}^b R_{defb} = g_{ej} g^{hc} (\Gamma^b{}_{ci} \Gamma^i{}_{ag} - \Gamma^b{}_{ai} \Gamma^i{}_{cg} - \partial_a \Gamma^b{}_{cg} + \partial_c \Gamma^b{}_{ag}) \\ &(-\Gamma^j{}_{dk} \Gamma^k{}_{bf} + \Gamma^j{}_{bk} \Gamma^k{}_{df} + \partial_b \Gamma^j{}_{df} - \partial_d \Gamma^j{}_{bf}) \end{aligned} \tag{A.7}$$

$$\begin{aligned} &- R_a{}^h{}_f{}^b R_{degb} = -g_{bj} g^{hc} (\Gamma^b{}_{ci} \Gamma^i{}_{af} - \Gamma^b{}_{ai} \Gamma^i{}_{cf} - \partial_a \Gamma^b{}_{cf} + \partial_c \Gamma^b{}_{af}) \\ &(\Gamma^j{}_{ek} \Gamma^k{}_{dg} - \Gamma^j{}_{dk} \Gamma^k{}_{eg} - \partial_d \Gamma^j{}_{eg} + \partial_e \Gamma^j{}_{dg}) \end{aligned} \tag{A.8}$$

$$\begin{aligned} &- R_a{}^h{}_d{}^b R_{ebfg} = -g_{bj} g^{hc} (\Gamma^b{}_{ci} \Gamma^i{}_{ad} - \Gamma^b{}_{ai} \Gamma^i{}_{cd} - \partial_a \Gamma^b{}_{cd} + \partial_c \Gamma^b{}_{ad}) \\ &(-\Gamma^j{}_{fk} \Gamma^k{}_{eg} + \Gamma^j{}_{ek} \Gamma^k{}_{fg} + \partial_e \Gamma^j{}_{fg} - \partial_f \Gamma^j{}_{eg}) \end{aligned} \tag{A.9}$$

and lastly, realizing that Eq. (A.6) cancels Eq. (A.7) using the relabelling $g \leftrightarrow e$, and Eq. (A.8) cancels Eq. (A.9) via $e \to f\,, f \to d\,, d \to e$.

Therefore, with the result in Eq. (A.3), and the result in Eq. (A.4) with exchanged covariant derivatives, the first term of the EOM Eq. (A.1) is recovered

$$8\,\epsilon^y{}_{bch} R^{zabc} (\nabla_a R^{defg}) (\nabla^h R_{defg}) + 8\,\epsilon^y{}_{bch} R^{defg} R^{zabc} (\nabla^h \nabla_a R_{defg}) = 4 \tilde{R}^{yazb} (\nabla_a \nabla_b \mathcal{C})\,. \tag{A.10}$$

The covariant derivatives of the term $4\,\epsilon_{efgh} R^{cdef} R^{yazb} (\nabla_b \nabla_a R_{cd}{}^{gh})$ can be exchanged. As in the result of Eq. (A.4), this can be proved by expanding the covariant derivative part, writing the resulting terms in terms of their Christoffel symbols, and performing the most convenient relabelling. Therefore,

$$\begin{aligned} &4\,\epsilon_{efgh} R^{cdef} R^{yazb} (\nabla_b \nabla_a R_{cd}{}^{gh}) + 4\,\epsilon_{efgh} R^{cdef} R^{yazb} (\nabla_a \nabla_b R_{cd}{}^{gh}) = \\ &= 8\,\epsilon_{efgh} R^{cdef} R^{yazb} (\nabla_a \nabla_b R_{cd}{}^{gh})\,. \end{aligned} \tag{A.11}$$

This result, along with the term $8\,\epsilon_{efgh} R^{yazb} (\nabla_a R^{cdef}) (\nabla_b R_{cd}{}^{gh})$ from the expansion, constitute the second term of the EOM Eq. (A.1)

$$8\,\epsilon_{efgh} R^{cdef} R^{yazb} (\nabla_a \nabla_b R_{cd}{}^{gh}) + 8\,\epsilon_{efgh} R^{yazb} (\nabla_a R^{cdef}) (\nabla_b R_{cd}{}^{gh}) = 4 R^{yazb} (\nabla_a \nabla_b \tilde{\mathcal{C}})\,. \tag{A.12}$$

By applying Eq. (3.26) from property i), and utilizing the symmetry of the metric, the following result is obtained

$$\begin{aligned} &2\,\epsilon^z{}_{ade} R_{bc}{}^{de} R_{fghi} R^{fghi} R^{yabc} + 2\,\epsilon^y{}_{ade} R_{bc}{}^{de} R_{fghi} R^{fghi} R^{zabc} = \\ &= \epsilon_{ghij} g^{yz} R_{abcd} R^{abcd} R_{ef}{}^{ij} R^{efgh}\,, \end{aligned} \tag{A.13}$$

which in turn cancels the term $-\epsilon_{ghij} g^{yz} R_{abcd} R^{abcd} R_{ef}{}^{ij} R^{efgh}$ from the expansion.

The last term of the EOM Eq. (A.1) is recovered by first applying the symmetries of the Levi-Civita and Riemann tensors to $2\epsilon g_{fghi} R_{de}{}^{hi} R^{defg} R^{yabc} R^{z}{}_{abc}$, followed by the application of Eq. (3.26) from property i).

Finally, after reproducing all the terms of the EOM, the following is left

$$\begin{aligned} &2\,\epsilon^{z}{}_{fgh} R_{abcd} R^{abcd} (\nabla_e \nabla^h R^{yefg}) + 2\,\epsilon^{y}{}_{fgh} R_{abcd} R^{abcd} (\nabla_e \nabla^h R^{zefg}) \\ &+ 4\,\epsilon^{z}{}_{fgh} R^{abcd} (\nabla_e R_{abcd}) (\nabla^h R^{yefg}) + 4\,\epsilon^{y}{}_{fgh} R^{abcd} (\nabla_e R_{abcd}) (\nabla^h R^{zefg})\,. \end{aligned} \tag{A.14}$$

This sum was proven to vanish by implementing it, along with the Kerr metric, with the numerical package xCoba, which allows evaluating any term on the basis of any metric.

Thus, it is proven that Eq. (A.1) is a simplification of Eq. (A.2), which in turn comes from applying EL to the eight-derivative correction $\mathcal{C}\tilde{\mathcal{C}}$.

B First-order perturbation of the Einstein tensor

This section sketches the first-order perturbation of the Einstein tensor for a general curved vacuum spacetime detailed in [23].

The derivation starts with the expansion of the Christoffel symbols

$$\begin{aligned} \Gamma^{a}_{bc} &= \frac{1}{2} g^{ad} \left(\partial_c g_{db} + \partial_b g_{dc} - \partial_d g_{bc}\right) = \\ &= \frac{1}{2} \left(g^{\mathrm{B}\,ad} - h^{ad}\right) \left(\partial_c g^{\mathrm{B}}_{db} + \partial_c h_{db} + \partial_b g^{\mathrm{B}}_{dc} + \partial_b h_{dc} - \partial_d g^{\mathrm{B}}_{bc} - \partial_d h_{bc}\right) + O(\varepsilon^2)\,. \end{aligned} \tag{B.15}$$

Then its perturbation reads

$$\begin{aligned} \Gamma^{a}_{bc} - \Gamma^{\mathrm{B}\,a}_{\ bc} = \delta\Gamma^{a}_{bc} &= -\frac{1}{2} h^{ad} g^{\mathrm{B}}_{de} \Gamma^{\mathrm{B}\,e}_{\ bc} + \frac{1}{2} g^{\mathrm{B}\,ad} \left(\partial_c h_{db} + \partial_b h_{dc} - \partial_d h_{bc}\right) = \\ &= \frac{1}{2} g^{\mathrm{B}\,ad} \left(\nabla^{\mathrm{B}}_c h_{db} + \nabla^{\mathrm{B}}_b h_{dc} - \nabla^{\mathrm{B}}_d h_{bc}\right). \end{aligned} \tag{B.16}$$

The Riemann tensor is then computed by applying Eq. (B.16) on its usual definition and evaluating the result at a point where $\Gamma^{\mathrm{B}\,a}_{\ bc} = 0$ [12]

$$R^{a}_{\ bcd} = \partial_c \Gamma^{a}_{bd} - \partial_d \Gamma^{a}_{bc} + \Gamma^{a}_{ce} \Gamma^{e}_{\ bd} - \Gamma^{a}_{de} \Gamma^{e}_{\ bc} = \partial_c \Gamma^{\mathrm{B}\,a}_{\ bd} - \partial_d \Gamma^{\mathrm{B}\,a}_{\ bc} + \partial_c \delta\Gamma^{a}_{bd} - \partial_d \delta\Gamma^{a}_{bc} + O(\varepsilon^2)\,. \tag{B.17}$$

Its perturbation at such point is then $\delta R^{a}_{\ bcd} = \partial_c \delta\Gamma^{a}_{bd} - \partial_d \delta\Gamma^{a}_{bc}$. Thus, by general covariance,

[12] The Local Flatness Theorem proves the existence of a transformation which converts any arbitrary coordinate system into another that reduces to an inertial system at a point $\mathcal{P}$ of a manifold. The metric near $\mathcal{P}$ is approximately η_{ab} , with $\partial_c g_{ab}(\mathcal{P}) = 0$ and $\partial_c \partial_d g_{ab}(\mathcal{P}) \neq 0$[24].

the perturbation of the Riemann tensor at an arbitrary coordinate system is

$$\delta R^{a}{}_{bcd} = \nabla^{\rm B}_{c}\delta\Gamma^{a}_{bd} - \nabla^{\rm B}_{d}\delta\Gamma^{a}_{bc} = \\ = \frac{1}{2}\left(\nabla^{\rm B}_{c}\nabla^{\rm B}_{b}h^{a}{}_{d} + \nabla^{\rm B}_{c}\nabla^{\rm B}_{d}h^{a}{}_{b} - \nabla^{\rm B}_{c}\nabla^{\rm B\,a}h_{bd} - \nabla^{\rm B}_{d}\nabla^{\rm B}_{b}h^{a}{}_{c} - \nabla^{\rm B}_{d}\nabla^{\rm B}_{c}h^{a}{}_{b} + \nabla^{\rm B}_{d}\nabla^{\rm B\,a}h_{bc}\right) . \tag{B.18}$$

The authors obtain the perturbations of the Ricci tensor and Ricci scalar using the usual contractions. Finally, by the convenient introduction of trace-reverse metric perturbation

$$\bar{h}_{ab} = h_{ab} - \frac{1}{2}g^{\rm B}_{ab}g^{\rm B\,cd}h_{cd}\,, \tag{B.19}$$

the authors arrive at the linearized vacuum EFE

$$\delta G_{bd} = -\frac{1}{2}\nabla^{\rm B}_{a}\nabla^{\rm B\,a}\bar{h}_{bd} + R^{\rm B}_{adbc}\bar{h}^{ac} - \frac{1}{2}g^{\rm B}_{bd}\nabla^{\rm B}_{a}\nabla^{\rm B}_{c}\bar{h}^{ac} + \frac{1}{2}\nabla^{\rm B}_{b}\nabla^{\rm B}_{a}\bar{h}^{a}{}_{d} + \frac{1}{2}\nabla^{\rm B}_{d}\nabla^{\rm B}_{a}\bar{h}^{a}{}_{b}\,. \tag{B.20}$$

C H_i functions in the metric corrections

H_i functions associated to the six-derivative corrections:

$$H_1^{(6)} = \lambda_{\rm ev}\left(-\frac{48M^3}{11r^7} + \frac{64}{231M^3r} - \frac{8M^2}{33r^6} - \frac{64}{231M^2r^2} - \frac{40M}{231r^5} - \frac{32}{231Mr^3} - \frac{32}{231r^4}\right) \\ + \lambda_{\rm odd}\chi x\left(-\frac{3456M^4}{91r^8} - \frac{1152M^3}{1001r^7} - \frac{96M^2}{143r^6} + \frac{768}{1001M^2r^2} - \frac{384M}{1001r^5} - \frac{192}{1001r^4}\right) + \mathcal{O}(\chi^2)\,, \tag{C.21}$$

$$H_2^{(6)} = \lambda_{\rm odd}\chi x\left(-\frac{1728M^3}{91r^7} - \frac{135}{1001M^3r} - \frac{6560M^2}{1001r^6} - \frac{948}{1001M^2r^2} - \frac{4040M}{1001r^5} - \frac{11112}{7007Mr^3} \right. \\ \left. - \frac{17676}{7007r^4}\right) + \lambda_{\rm ev}\left(\frac{32}{231M^4} - \frac{32}{231M^3r} - \frac{24M^2}{11r^6} - \frac{16}{231M^2r^2} - \frac{4M}{33r^5} - \frac{16}{231Mr^3} \right. \\ \left. - \frac{20}{231r^4}\right) + \mathcal{O}(\chi^2)\,, \tag{C.22}$$

$$H_3^{(6)} = \lambda_{\rm odd}\chi x\left(-\frac{19008M^3}{91r^7}+\frac{4320M^2}{1001r^6}+\frac{768}{1001M^2r^2}+\frac{384M}{143r^5}+\frac{1152}{1001Mr^3}+\frac{1728}{1001r^4}\right)$$
$$+\lambda_{\rm ev}\left(-\frac{64}{231M^4}+\frac{64}{231M^3r}-\frac{392M^2}{11r^6}+\frac{32}{231M^2r^2}+\frac{8M}{33r^5}+\frac{32}{231Mr^3}+\frac{40}{231r^4}\right)+\mathcal{O}(\chi^2)\,, \tag{C.23}$$

$$H_4^{(6)} = \lambda_{\rm odd}\chi x\left(-\frac{19008M^3}{91r^7}+\frac{4320M^2}{1001r^6}+\frac{768}{1001M^2r^2}+\frac{384M}{143r^5}+\frac{1152}{1001Mr^3}+\frac{1728}{1001r^4}\right)$$
$$+\lambda_{\rm ev}\left(-\frac{64}{231M^4}+\frac{64}{231M^3r}-\frac{392M^2}{11r^6}+\frac{32}{231M^2r^2}+\frac{8M}{33r^5}+\frac{32}{231Mr^3}+\frac{40}{231r^4}\right)+\mathcal{O}(\chi^2)\,, \tag{C.24}$$

H_i functions associated to the eight-derivative corrections:

$$H_1^{(8)} = \epsilon_3\chi x\left(\frac{799488M^5}{95r^{11}}-\frac{7471488M^4}{1615r^{10}}+\frac{49152}{20995M^4r^2}-\frac{16896M^3}{1615r^9}\right.$$
$$\left.-\frac{25344M^2}{4199r^8}-\frac{12288}{20995M^2r^4}-\frac{73728M}{20995r^7}-\frac{24576}{20995Mr^5}-\frac{43008}{20995r^6}\right)+\epsilon_1\left(\frac{16384}{12155M^5r}\right.$$
$$+\frac{32512M^4}{17r^{10}}-\frac{16384}{12155M^4r^2}-\frac{87424M^3}{85r^9}-\frac{8192}{12155M^3r^3}-\frac{3072M^2}{1105r^8}-\frac{8192}{12155M^2r^4}$$
$$\left.-\frac{21504M}{12155r^7}-\frac{2048}{2431Mr^5}-\frac{14336}{12155r^6}\right)+\mathcal{O}(\chi^2)\,, \tag{C.25}$$

$$H_2^{(8)} = -\frac{6912M^2\epsilon_2}{11r^8}+\epsilon_3\chi x\left(-\frac{326811}{419900M^5r}+\frac{399744M^4}{95r^{10}}-\frac{354697}{104975M^4r^2}-\frac{170368M^3}{1615r^9}\right.$$
$$\left.-\frac{813842}{146965M^3r^3}-\frac{100576M^2}{1615r^8}-\frac{257055}{29393M^2r^4}-\frac{3909792M}{104975r^7}-\frac{878354}{62985Mr^5}-\frac{7118992}{314925r^6}\right)$$
$$+\epsilon_1\left(\frac{8192}{12155M^6}-\frac{8192}{12155M^5r}-\frac{4096}{12155M^4r^2}+\frac{16256M^3}{17r^9}-\frac{4096}{12155M^3r^3}-\frac{589632M^2}{935r^8}\right.$$
$$\left.-\frac{1024}{2431M^2r^4}-\frac{1536M}{1105r^7}-\frac{7168}{12155Mr^5}-\frac{10752}{12155r^6}\right)+\mathcal{O}(\chi^2)\,, \tag{C.26}$$

$$H_3^{(8)} = \epsilon_3\chi x\bigg(-\frac{208512M^4}{95r^{10}} + \frac{49152}{20995M^4r^2} + \frac{101376M^3}{1615r^9} + \frac{73728}{20995M^3r^3} + \frac{59136M^2}{1615r^8} + \frac{110592}{20995M^2r^4} + \frac{456192M}{20995r^7} + \frac{172032}{20995Mr^5} + \frac{55296}{4199r^6}\bigg) + \epsilon_1\bigg(-\frac{16384}{12155M^6} + \frac{16384}{12155M^5r} + \frac{8192}{12155M^4r^2} - \frac{8576M^3}{17r^9} + \frac{8192}{12155M^3r^3} + \frac{384M^2}{85r^8} + \frac{2048}{2431M^2r^4} + \frac{3072M}{1105r^7} + \frac{14336}{12155Mr^5} + \frac{21504}{12155r^6}\bigg) + \mathcal{O}(\chi^2)\,, \tag{C.27}$$

$$H_4^{(8)} = \epsilon_3\chi x\bigg(-\frac{208512M^4}{95r^{10}} + \frac{49152}{20995M^4r^2} + \frac{101376M^3}{1615r^9} + \frac{73728}{20995M^3r^3} + \frac{59136M^2}{1615r^8} + \frac{110592}{20995M^2r^4} + \frac{456192M}{20995r^7} + \frac{172032}{20995Mr^5} + \frac{55296}{4199r^6}\bigg) + \epsilon_3\bigg(-\frac{16384}{12155M^6} + \frac{16384}{12155M^5r} + \frac{8192}{12155M^4r^2} - \frac{8576M^3}{17r^9} + \frac{8192}{12155M^3r^3} + \frac{384M^2}{85r^8} + \frac{2048}{2431M^2r^4} + \frac{3072M}{1105r^7} + \frac{14336}{12155Mr^5} + \frac{21504}{12155r^6}\bigg) + \mathcal{O}(\chi^2)\,. \tag{C.28}$$

D Coefficients of the corrected Kerr Black Hole's properties

Coefficients $\Delta\Omega_H^{(i,j)}$ from the angular velocity in the three-term notation Eq. (5.63):

$$\Delta\Omega_H^{(6,\mathrm{ev})} = \frac{5\chi}{32} + \frac{1}{64}\chi^3 + \frac{3}{448}\chi^5 + \frac{11}{1792}\chi^7 + \frac{377}{57344}\chi^9 + \frac{115}{16384}\chi^{11} + \mathcal{O}(\chi^{13})\,, \tag{D.1}$$

$$\Delta\Omega_H^{(8,1)} = \frac{35\chi}{176} - \frac{35623}{46760}\chi^3 + \frac{41772}{45760}\chi^5 - \frac{2630965}{2489344}\chi^7 - \frac{1128466969}{945950720}\chi^9 + \mathcal{O}(\chi^{11})\,, \tag{D.2}$$

$$\Delta\Omega_H^{(8,2)} = \frac{-108\chi}{176} - \frac{7452}{45760}\chi^3 - \frac{24183}{45760}\chi^5 - \frac{2020784}{2489344}\chi^7 - \frac{967867816}{945950720}\chi^9 + \mathcal{O}(\chi^{11})\,. \tag{D.3}$$

Coefficients $\Delta\kappa^{(i,j)}$ from the surface gravity in the three-term notation Eq. (5.67):

$$\Delta\kappa^{(6,\mathrm{ev})} = \frac{1}{32} - \frac{7}{64}\chi^2 - \frac{3}{64}\chi^4 - \frac{7}{256}\chi^6 - \frac{157}{8192}\chi^8 + \mathcal{O}\left(\chi^{10}\right), \tag{D.4}$$

$$\Delta\kappa^{(8,1)} = \frac{1}{8} - \frac{3}{22}\chi^2 + \frac{12083}{22880}\chi^4 + \frac{13303}{16640}\chi^6 + \frac{24673533}{24893440}\chi^8 + \mathcal{O}\left(\chi^{10}\right), \tag{D.5}$$

$$\Delta\kappa^{(8,2)} = \frac{27}{44}\chi^2 + \frac{8937}{22880}\chi^4 + \frac{291}{520}\chi^6 + \frac{4763873}{6223360}\chi^8 + \mathcal{O}\left(\chi^{10}\right), \tag{D.6}$$

Coefficients $\Delta A^{(i,j)}$ from the horizon area in the three-term notation Eq. (5.71):

$$\Delta A^{(6,\mathrm{ev})} = \frac{(1+\sqrt{1-\chi^2})}{143360}\left[-716800 + 107520\chi^2 + 105728\chi^4 + 78080\chi^6 + \mathcal{O}\left(\chi^8\right)\right] \tag{D.7}$$

$$\begin{aligned}\Delta A^{(8,1)} = \frac{(1+\sqrt{1-\chi^2})}{600865475710156800}\big[&- 6008654757101568000 - 54624134155468800\chi^2 \\ &- 2074876726613114880\chi^4 - 2771754622742691840\chi^6 + \mathcal{O}\left(\chi^8\right)\big]\end{aligned} \tag{D.8}$$

$$\begin{aligned}\Delta A^{(8,2)} = \frac{(1+\sqrt{1-\chi^2})\,\chi^2}{150216368927539200}\big[&- 1966468829596876800 - 1555212127253299200\chi^2 \\ &- 1271271676056698880\chi^4 - 1048870270794792960\chi^6 + \mathcal{O}\left(\chi^8\right)\big]\end{aligned} \tag{D.9}$$

Coefficients $\Delta\rho^{(i,j)}$ from the ergosphere radious in the three-term notation Eq. (5.81):

$$\Delta\rho^{(6,\mathrm{ev})} = \chi^2(1-x^2)\frac{1}{2} + \chi^4(1-x^2)\left(\frac{1245x^2}{5096} + \frac{3243}{10192}\right) + \mathcal{O}(\chi^6) \tag{D.10}$$

$$\Delta\rho^{(6,\mathrm{odd})} = \chi^5 x(1-x^2)\left(\frac{669}{106624} - \frac{669x^2}{106624}\right) + \mathcal{O}(\chi^7), \tag{D.11}$$

$$\Delta\rho^{(8,1)} = -\chi^2(x^2-1)\frac{13}{44} + \chi^4(x^2-1)\frac{(-197994203 + 806487443x^2)}{221707200} + \mathcal{O}(\chi^6) \tag{D.12}$$

$$\Delta\rho^{(6,2)} = \chi^2(x^2-1)\frac{27}{11} + \chi^4(x^2-1)\frac{(3(-110545633 + 431245873x^2))}{58658400} + \mathcal{O}(\chi^6) \tag{D.13}$$

$$\Delta\rho^{(6,3)} = \chi^5(x^2-1)^2\frac{35563903x}{1372879200} + \chi^7 x(x^2-1)^2\frac{(84116305 + 78492971x^2)}{8398790400} + \mathcal{O}(\chi^9) \tag{D.14}$$

References

[1] Clifford M. Will. "The Confrontation between General Relativity and Experiment". In: *Living Reviews in Relativity* 17.1 (June 2014). ISSN: 1433-8351. DOI: 10.12942/lrr-2014-4. URL: http://dx.doi.org/10.12942/lrr-2014-4.

[2] B. P. Abbott et al. "Observation of Gravitational Waves from a Binary Black Hole Merger". In: *Phys. Rev. Lett.* 116 (6 Feb. 2016), p. 061102. DOI: 10.1103/PhysRevLett.116.061102. URL: https://link.aps.org/doi/10.1103/PhysRevLett.116.061102.

[3] The Event Horizon Telescope Collaboration et al. "First M87 Event Horizon Telescope Results. I. The Shadow of the Supermassive Black Hole". In: *The Astrophysical Journal Letters* 875.1 (Apr. 2019), p. L1. DOI: 10.3847/2041-8213/ab0ec7. URL: https://dx.doi.org/10.3847/2041-8213/ab0ec7.

[4] James Owen Weatherall. *Where Does General Relativity Break Down?* 2022. arXiv: 2204.03869 [physics.hist-ph].

[5] John Earman and Jean Eisenstaedt. "Einstein and Singularities". In: *Studies in History and Philosophy of Science Part B: Studies in History and Philosophy of Modern Physics* 30.2 (1999), pp. 185–235. ISSN: 1355-2198. DOI: https://doi.org/10.1016/S1355-2198(99)00005-2. URL: https://www.sciencedirect.com/science/article/pii/S1355219899000052.

[6] Pablo A. Cano and Alejandro Ruipérez. "Leading higher-derivative corrections to Kerr geometry". In: *JHEP* 05 (2019). [Erratum: JHEP 03, 187 (2020)], p. 189. DOI: 10.1007/JHEP05(2019)189. arXiv: 1901.01315 [gr-qc].

[7] https://www.ligo.org/credits.php. *LIGO Scientific Collaboration*. URL: https://www.ligo.org/ (visited on 07/05/2024).

[8] *VIRGO*. URL: https://www.virgo-gw.eu/ (visited on 07/05/2024).

[9] *Event Horizon Telescope*. URL: https://eventhorizontelescope.org/ (visited on 07/05/2024).

[10] Vitor Cardoso et al. "Black Holes in an Effective Field Theory Extension of General Relativity". In: *Physical Review Letters* 121.25 (Dec. 2018). ISSN: 1079-7114. DOI: 10.1103/physrevlett.121.251105. URL: http://dx.doi.org/10.1103/PhysRevLett.121.251105.

[11] Ariel Edery and Benjamin Constantineau. "Extremal black holes, gravitational entropy and nonstationary metric fields". In: *Classical and Quantum Gravity* 28.4 (Jan. 2011), p. 045003. ISSN: 1361-6382. DOI: 10.1088/0264-9381/28/4/045003. URL: http://dx.doi.org/10.1088/0264-9381/28/4/045003.

[12] Pablo A. Cano et al. "Black hole multipoles in higher-derivative gravity". In: *Journal of High Energy Physics* 2022.12 (Dec. 2022). ISSN: 1029-8479. DOI: 10.1007/jhep12(2022)120. URL: http://dx.doi.org/10.1007/JHEP12(2022)120.

[13] Emmanuel N. Saridakis et al. *Modified Gravity and Cosmology: An Update by the CANTATA Network*. 2023. arXiv: 2105.12582 [gr-qc].

[14] José Alberto Orejuela García. *Lovelock Theories as extensions to General Relativity*. Tesis Univ. Granada., 2020. URL: http://hdl.handle.net/10481/63513.

[15] Solomon Endlich et al. "An effective formalism for testing extensions to General Relativity with gravitational waves". In: *Journal of High Energy Physics* 2017.9 (Sept. 2017). ISSN: 1029-8479. DOI: 10.1007/jhep09(2017)122. URL: http://dx.doi.org/10.1007/JHEP09(2017)122.

[16] José M. Martín-García. *xTensor: Fast abstract tensor computer algebra*. URL: http://xact.es/xTensor/ (visited on 10/05/2024).

[17] Teake Nutma. "xTras: A field-theory inspired xAct package for mathematica". In: *Computer Physics Communications* 185.6 (June 2014), pp. 1719–1738. ISSN: 0010-4655. DOI: 10.1016/j.cpc.2014.02.006. URL: http://dx.doi.org/10.1016/j.cpc.2014.02.006.

[18] David Yllanes and José M. Martín-García. *xCoba: General component tensor computer algebra*. URL: http://xact.es/xCoba/ (visited on 07/05/2024).

[19] Leo C. Stein. *Note on a (dimension-dependent) Weyl identity*. 2017. URL: https://duetosymmetry.com/notes/note-on-a-dimension-dependent-Weyl-identity/ (visited on 09/02/2017).

[20] Giovanni Catino and Paolo Mastrolia. "The Weyl Tensor". In: *A Perspective on Canonical Riemannian Metrics*. Cham: Springer International Publishing, 2020, pp. 51–70. ISBN: 978-3-030-57185-6. DOI: 10.1007/978-3-030-57185-6_3. URL: https://doi.org/10.1007/978-3-030-57185-6_3.

[21] Roger Penrose and Wolfgang Rindler. "Differentiation and curvature". In: *Spinors and Space-Time*. Cambridge Monographs on Mathematical Physics. Cambridge University Press, 1984, pp. 179–311.

[22] David Brizuela, Jose M. Martin-Garcia, and Guillermo A. Mena Marugan. "xPert: Computer algebra for metric perturbation theory". In: *Gen. Rel. Grav.* 41 (2009), pp. 2415–2431. DOI: 10.1007/s10714-009-0773-2. arXiv: 0807.0824 [gr-qc].

[23] Éanna É Flanagan and Scott A Hughes. "The basics of gravitational wave theory". In: *New Journal of Physics* 7 (Sept. 2005), pp. 204–204. ISSN: 1367-2630. DOI: 10.1088/1367-2630/7/1/204. URL: http://dx.doi.org/10.1088/1367-2630/7/1/204.

[24] Bernard Schutz. *A First Course in General Relativity*. 3rd ed. Cambridge University Press, 2022.

[25] Robert M. Wald. "Black Holes and Thermodynamics". In: *Black Hole Physics*. Ed. by Venzo De Sabbata and Zhenjiu Zhang. Dordrecht: Springer Netherlands, 1992, pp. 55–97. ISBN: 978-94-011-2420-1. DOI: 10.1007/978-94-011-2420-1_2. URL: https://doi.org/10.1007/978-94-011-2420-1_2.

[26] James M. Bardeen, B. Carter, and S. W. Hawking. "The Four laws of black hole mechanics". In: *Commun. Math. Phys.* 31 (1973), pp. 161–170. DOI: 10.1007/BF01645742.

[27] B Carter. "KILLING HORIZONS AND ORTHOGONALLY TRANSITIVE GROUPS IN SPACE–TIME." In: *J. Math. Phys. (N.Y.), 10: 70-81(Jan. 1969).* (Jan. 1969). DOI: 10.1063/1.1664763. URL: https://www.osti.gov/biblio/4824616.

[28] Eric Poisson. *A Relativist's Toolkit: The Mathematics of Black-Hole Mechanics*. Cambridge University Press, 2009.

[29] Sayantani Bhattacharyya et al. "The zeroth law of black hole thermodynamics in arbitrary higher derivative theories of gravity". In: *Journal of High Energy Physics* 2022.10 (Oct. 2022). ISSN: 1029-8479. DOI: 10.1007/jhep10(2022)013. URL: http://dx.doi.org/10.1007/JHEP10(2022)013.

[30] Roger Penrose. "The question of cosmic censorship". In: *J. Astrophys. Astron.* 20 (1999), pp. 233–248. DOI: 10.1007/BF02702355.

[31] Alexandre Le Tiec, Marc Casals, and Edgardo Franzin. "Tidal Love numbers of Kerr black holes". In: *Physical Review D* 103.8 (Apr. 2021). ISSN: 2470-0029. DOI: 10.1103/physrevd.103.084021. URL: http://dx.doi.org/10.1103/PhysRevD.103.084021.

[32] Pablo A. Cano et al. "Universal Teukolsky equations and black hole perturbations in higher-derivative gravity". In: *Physical Review D* 108.2 (July 2023). ISSN: 2470-0029. DOI: 10.1103/physrevd.108.024040. URL: http://dx.doi.org/10.1103/PhysRevD.108.024040.

[33] Dongjun Li et al. "Perturbations of Spinning Black Holes beyond General Relativity: Modified Teukolsky Equation". In: *Physical Review X* 13.2 (May 2023). ISSN: 2160-3308. DOI: 10.1103/physrevx.13.021029. URL: http://dx.doi.org/10.1103/PhysRevX.13.021029.